Differentially expressed genes in mycorrhized and nodulated roots of common bean are associated with defense, cell wall architecture, N metabolism, and P metabolism

Kalpana Nanjareddy[1☯], **Manoj-Kumar Arthikala**[1☯]*, **Brenda-Mariana Gómez**[1],
Lourdes Blanco[1,2], **Miguel Lara**[1,3]

1 Ciencias Agrogenómicas, Escuela Nacional de Estudios Superiores Unidad León- Universidad Nacional
Autónoma de México (UNAM), León, Guanajuato, México, **2** Instituto de Fisiología Celular, Universidad
Nacional Autónoma de México (UNAM), Ciudad Universitaria, Coyoacan, Ciudad de México, México,
3 Instituto de Biología, Universidad Nacional Autónoma de México (UNAM), Ciudad Universitaria, Coyoacan,
Ciudad de México, México

☯ These authors contributed equally to this work.
* manojarthik@gmail.com

Abstract

Legumes participate in two important endosymbiotic associations, with phosphorus-acquiring
arbuscular mycorrhiza (AM, soil fungi) and with nitrogen-fixing bacterial rhizobia. These diver-
gent symbionts share a common symbiotic signal transduction pathway that facilitates the
establishment of mycorrhization and nodulation in legumes. However, the unique and shared
downstream genes essential for AM and nodule development have not been identified in crop
legumes. Here, we used ion torrent next-generation sequencing to perform comparative tran-
scriptomics of common bean (*Phaseolus vulgaris*) roots colonized by AM or rhizobia. We ana-
lyzed global gene expression profiles to identify unique and shared differentially expressed
genes (DEGs) that regulate these two symbiotic interactions, and quantitatively compared
DEG profiles. We identified 3,219 (1,959 upregulated and 1,260 downregulated) and 2,645
(1,247 upregulated and 1,398 downregulated) unigenes that were differentially expressed in
response to mycorrhizal or rhizobial colonization, respectively, compared with uninoculated
roots. We obtained quantitative expression profiles of unique and shared genes involved in
processes related to defense, cell wall structure, N metabolism, and P metabolism in mycor-
rhized and nodulated roots. KEGG pathway analysis indicated that most genes involved in
jasmonic acid and salicylic acid signaling, N metabolism, and inositol phosphate metabolism
are variably expressed during symbiotic interactions. These combined data provide valuable
information on symbiotic gene signaling networks that respond to mycorrhizal and rhizobial
colonization, and serve as a guide for future genetic strategies to enhance P uptake and N-fix-
ing capacity to increase the net yield of this valuable grain legume.

Introduction

Legumes have the unique capacity to form symbiotic associations with ancient phosphorus-acquiring arbuscular mycorrhizal fungi (AMF, which arose ~450 million years ago) and recent nitrogen-fixing *Rhizobium* bacteria (which arose ~60 million years ago) in a tripartite relationship [1–4]. AMF belonging to the phylum Glomeromycota help their host plants absorb and translocate the major mineral nutrients phosphorus (P) and nitrogen (N) and minor micronutrients from the soil [5]. Nitrogen-fixing rhizobial bacteria convert atmospheric free nitrogen to ammonia, which the host plant uses for growth and development [6]. In return, the host plant provides the micro-symbionts with photosynthetically fixed carbon compounds [7]. The symbiotic interaction is initiated by a molecular dialogue between the host and AMF or rhizobial partners, which functions to establish a mutually beneficial relationship without invoking host plant defenses. These initial interactions include complex signal perception and transduction networks governed by regulatory genes in both symbiotic partners. In response to plant-derived bioactive signals such as strigolactones [8] and (iso)flavonoids, AMF and rhizobia synthesize and secrete Myc (lipochitooligosaccharide (LCO) [9] and short-chain chitin oligomer (COS) [10]) and Nod (LCO [11]) factors, respectively. The Myc and Nod factors stimulate signaling by a common symbiosis pathway (CSP), which is shared between AMF and rhizobial symbioses [12].

Plant genes and proteins involved in the initial symbiotic signaling interactions were identified and temporally ordered by performing systematic phenotypic analyses of model legume (*Lotus japonicus* and *Medicago truncatula*) mutants arrested at different stages of the symbiotic response [13,14]. The CSP genes such as SYMRK, CASTOR, POLLUX, NUP85, and NUP133 are required for the induction of calcium spiking, a distinctive physiological response during early symbiotic interactions. CALCIUM- AND CALMODULIN-DEPENDENT PROTEIN KINASE (CCAMK, a decoder of calcium signaling) and CYCLOPS are downstream of calcium spiking [12]. In a downstream or parallel event, the GRAS protein transcription factors NSP1, NSP2 [15,16], and RAM1 [17] form complexes that drive symbiont-specific gene expression in legumes. For example, RAM1 and RAM2 induce the biosynthesis of cutin monomers, which are involved in appressorium formation by AMF [18]. NSP1 and NSP2 are sufficient to activate the nodulation-specific ERF transcription factor ERN1 [19] and the downstream transcription factors NIN, NF-YA, and NF-YB, which are involved in the initiation of nodule organogenesis [20,21] along with cytokinin signaling factors [22,23]. Subsequently, the host plant enables colonization by either AMF or rhizobia, depending on its perception of early bioactive signals. Nevertheless, for the successful colonization of these symbionts the legume plants must avoid eliciting defense responses and compromise for cell wall degradation during invasion [24]. Indeed, a transient induction of few defense markers show at early stages of symbionts interactions suggesting that general microbe-associated molecular patterns from AM fungi or rhizobia are perceived and elicit an ephemeral defense response, which later is suppressed [24]. Proteins involved in the blocking this defense pathway and cell wall loosening associated enzymes are poorly understood.

Common bean (*Phaseolus vulgaris*) is the most important crop grain legume and is a rich source of dietary protein. *P. vulgaris* participates in both AMF and root nodule symbiosis. RNA interference (RNAi) studies have functionally validated several genes associated with nodule symbiosis in *P. vulgaris*, such as the heterotrimeric nuclear factor-YC1 (PvNF-YC1) [25], PvNF-YB [21], PvSYMRK [26], PvRACK1 [27], PvNADPH-OXIDASE [28], PvTRE1 [29], PvNODULIN 22 [30], PvSIN1 [31], and PvTOR [32]. The functions of most of these genes have not been determined in AMF symbiotic interactions. Several recent studies described the functions of *Pv*RBOHB [33,34] and an autophagy-related kinase [35] during

AMF symbiosis. However, plant genes that participate in AMF symbiosis are still largely unidentified. Therefore, further research is required to investigate and identify novel genes associated with AMF and root nodule symbioses in common bean. High-throughput technologies such as microarray analysis and next-generation sequencing have been used to examine differential gene expression patterns under AMF and rhizobial symbiotic conditions by performing comparative transcriptome profiling in model legumes [36,37,38,39]. However, these analyses have not been performed in important crop grain legumes. Comparative transcriptome analyses were performed previously using cDNA macroarrays in *L. japonicas* [36] and microarrays in *Casuarina glauca* and *M. truncatula* symbiotic roots [37]. Rapid advances in RNA-sequencing (RNA-Seq) and associated bioinformatics strategies have provided revolutionary tools for global transcriptomic research on plants [40]. For example, these tools have been used to elucidate gibberellin biosynthesis gene expression patterns [41] and transcription factors [42] associated with mycorrhizal colonization.

In the present study, we analyzed transcriptome changes in *P. vulgaris* roots under AMF and nodulated conditions using RNA-Seq technology. Our root transcriptional analysis identified 3,219 and 2,645 genes that were differentially expressed in response to mycorrhizal or rhizobial colonization, respectively. These data were used to predict key modules that control these two divergent root symbionts such as defense response, cell wall integrity, N metabolism and P metabolism. Further, we performed a comparative and quantitative analyses of host gene expression profiles associated with defense, cell wall structure, N metabolism and P metabolism.

Materials and methods

Plant materials, symbiont inoculation, and growth conditions

Phaseolus vulgaris L. cv. Negro Jamapa seeds obtained from Instituto de Biotecnología, UNAM, Mexico were used for all experiments. Seeds were surface-sterilized by immersion in absolute ethanol for 1 min and 10% sodium hypochlorite for 10 min, followed by three washes with sterile distilled water. Then, seeds were germinated on sterile filter paper moistened with B&D solution [43] in darkness for 2 days at 28°C. Two-day-old germinated seeds were planted in pots containing sterile vermiculite, and maintained under greenhouse conditions with a 16-h photoperiod and 65% relative humidity at 27±1°C. Five-day-old seedlings (n = 9 for each set) were inoculated in the root zone with 1 ml of *Rhizophagus irregularis* spores (1,000 spores/seedling) [Symplanta®, Germany], or *Rhizobium tropici* strain CIAT899 (1 ml/seedling at OD_{600} = 0.05) dx.doi.org/10.17504/protocols.io.h83b9yn. The choice of *R. irregularis* and *R. tropici* for this study is both are the most studied symbionts and these species are tolerant of stress conditions such as high temperature and acidity [44,45]. Inoculated seedlings were irrigated two times per week with modified B&D solution to promote mycorrhizal colonization (supplemented with 10 μM potassium phosphate [46]) or to promote nodulation (B&D solution without nitrate [47]). A set (n = 9) of uninoculated plants grown separately under identical conditions was used as the control (S1 Fig). At different time points (1, 2, 3 wpi), root samples (3 plants from each set, approximately 3 g) were excised from these plants (*R. irregularis*, *R. tropici*, and control), and half of the sample was immediately frozen in liquid nitrogen and stored at -80°C for RNA extraction. The remaining half of the sample was used for further analyses such as, calculation of %RLC and quantification phosphorous in mycorrhized and nitrogenase assay in rhizobia inoculated roots, RT-qPCR to confirm the symbiosis and validate the RNA-Seq data.

Based on the PvPT4 expression in AMF inoculated and nitrogen fixing ability and absence of senescenced nodules in rhizobia inoculated roots, 2 wpi roots were selected for transcriptome analysis.

Assessment of mycorrhization and nodulation

To determine the status of mycorrhizal colonization, the remaining mycorrhized root samples were stained using a modified trypan blue histochemical staining method. Stained root samples were examined under a light microscope (Leica, DMLB bright-field microscope) to visualize fungal structures and determine the percentage of root length colonization (%RLC) according to McGonigle et al. [48]. Total phosphorus concentration in dried leaves was measured using the nitric-perchloric acid method following the protocol described by Miller [49]. The acid-digested samples were dissolved in distilled water and quantified spectrophotometrically. A standard curve was prepared using KH_2PO_4. In parallel, ethylene production in nodulated root samples was quantified by subjecting samples to the acetylene reduction assay described previously by Ramírez et al. [50]. The samples were incubated in acetylene gas for 30 min, and ethylene production was determined by gas chromatography (Variant model 3300). Ethylene specific activity was expressed as $\mu l\ mol^{-1}\ C_2H_2\ h^{-1}\ g^{-1}$ of nodule dry weight (DW).

Quantitative real-time PCR analysis

The RT-qPCR analysis was performed to verify the absence of mycorrhiza and rhizobia cross contamination; and also to validate the RNA-Seq data (S1 Table). Six genes each for mycorrhized and nodulated conditions were selected to validate the RNA-Seq data among which, two genes were symbiosis specific, two genes that were highly upregulated and two genes that were highly downregulated. High-quality total RNA was isolated from frozen root tissues using TRIzol reagent (Sigma) according to the manufacturer's instructions. RNA integrity was verified by gel electrophoresis, and RNA concentration was assessed using a NanoDrop spectrophotometer (Thermo Scientific). DNA contamination was eliminated using RNase-free DNase (1 U/µl; Roche, USA) according to the manufacturer's instructions. Reverse-transcription quantitative PCR (RT-qPCR) analysis was performed using a DNA-free RNA and iScript^{TM} One-Step RT-PCR Kit with SYBR$^{®}$ Green (Bio-Rad) according to the manufacturer's instructions. A control sample lacking reverse transcriptase was included to confirm the absence of contaminant DNA. Relative expression values were calculated using the $2^{-\Delta Ct}$ method, where the quantification cycle (Cq) value equals the Cq value of the gene of interest minus the Cq value of the reference gene [51]. Gene-specific primers were used for RT-qPCR analysis (S1 Table). The *Phaseolus vulgaris* genes EF1α and IDE were used as reference as described previously by Arthikala et al. [33]. The relative expression values were normalized with respect to two reference genes EF1α and IDE as described previously by Vandesompele et al. [52]. The presented values are averages of three biological replicates, and each data set was recorded using triplicate samples.

Transcriptome analysis

mRNA enrichment. For transcriptome profiling, high-quality total RNA was isolated from frozen root tissues from two biological replicates using the RNeasy® Plant Mini Kit according to the manufacturer's instructions (Qiagen, Hilden, Germany). Genomic DNA contamination was eliminated by incubating the samples with RNase-free DNase (1 U μl^{-1}) at 37˚C for 15 min, and then at 65˚C for 10 min. RNA quality was tested by measuring the A_{260}/A_{280} and A_{260}/A_{230} ratios using a NanoDrop Spectrophotometer. Electropherograms were obtained using an Agilent 2100 Bioanalyzer platform (Agilent Technologies, USA) with an Agilent RNA 6000 Nano Kit; Agilent 2100 Expert software version B.02.03.SI307 was used to calculate the RNA integrity number (RIN) [53]. RIN values of samples ranged from 7.0 to 7.5. A 1 µg aliquot of total RNA was subjected to mRNA enrichment using the Dynabeads® mRNA DIRECT™ Micro Kit (Cat. nr. 61021, Life Technologies) according to the manufacturer's instructions.

Library preparation. The cDNA libraries were constructed using the Ion Total RNA-Seq Kit v2 (Cat. nr. 4479789, Life Technologies) according to the manufacturer's instructions. Briefly, 100 ng of enriched mRNA was fragmented for 10 min with RNase III. Fragmented RNA was purified using nucleic acid binding beads and binding buffers according to the manufacturer's instructions (Cat. nr. 4475486, Life Technologies). Purified samples were evaluated on an Agilent 2100 Bioanalyzer to assess yield and mRNA fragment size distribution. Then, 25–50 ng of fragmented mRNA was hybridized with ion adapters in a thermocycler for 10 min at 65°C and 5 min at 30°C. Hybridized fragmented mRNA was incubated with ligase (Cat. nr. AM2141, Life Technologies) for 30 min at 30°C to ligate the adapters. Then, the hybridized samples were mixed with reverse transcriptase master mix, and incubated at 42°C for 30 min to generate cDNA libraries. The cDNA libraries were purified using nucleic acid binding beads and buffers according to the manufacturer's standardized protocol (Cat. nr. 4475486, Life Technologies). The purified cDNA libraries were subjected to PCR amplification using Platinum PCR Supermix High Fidelity and Ion Xpress Barcode reverse and forward primers (Thermo Fisher Scientific) with the following conditions: 95°C for 2 min; two cycles of 94°C for 30 s, 50°C for 30 s, and 68°C for 30 s; 14 cycles of 94°C for 30 s, 62°C for 30 s, and 68°C for 30 s; and a final extension at 68°C for 5 min. The amplified cDNA libraries were purified using nucleic acid binding beads and binding buffers. The yield and size distribution of each library were evaluated using the Agilent 2100 Bioanalyzer.

Template preparation, enrichment, and sequencing. Templates were prepared from 10 pM of pooled barcoded cDNA libraries using the Ion PI Template OT2 Solutions 200 Kit v3 (Cat. nr. 4488318, Life Technologies) according to the manufacturer's instructions. Briefly, 10 pM of pooled cDNA libraries was mixed with Ion PI reagent mix TL, Ion PI PCR reagent B, Ion PI enzyme mix TL, and Ion PI Ion sphere particles v3. The mixtures were vortexed, transferred into an Ion PI Plus reaction filter assembly, and then the assemblies were loaded in the Ion OneTouch 2 instrument for template amplification (Life Technologies). The instrument was turned on and the reactions ran for 6.5 h. Then, the beads were isolated and quality was assessed on a QuBit instrument to determine the percent of beads that contained polyclonal templates. After polyclonal assessment, the samples were enriched using the reagents in the Ion PI Template OT2 Solutions 200 Kit v3 (Cat. nr. 4488318, Life Technologies) and the Ion OneTouch ES instrument, according to the manufacturer's instructions. After enrichment, the beads were washed and prepared for sequencing. Then, the beads were loaded onto a prepared and calibrated Ion P1 Chip (Life Technologies) according to the manufacturer's Ion P1 Sequencing 200 Kit v3 protocol. The loaded chip was placed into the Ion Proton Sequencer, and the run was started using an Ion Torrent RNA-Seq run plan that was configured based on the library type, species, required number of run flows, required type of plug-in, adapter trimming, and other parameters that were specific for the RNA-Seq run. RNA sequencing and analysis were performed by the PrimBio Research Institute LLC, Exton, PA, USA.

Alignment and data analysis. After the proton run was completed, the raw sequences were aligned to *R. irregularis / R. tropici* database to eliminate the transcripts aligned to the symbiont's database (http://fungi.ensembl.org/Rhizophagus_irregularis_daom_197198w/Info/Index, http://genome.annotation.jp/RhizoBase). Next, the filtered sequences were aligned to the *P. vulgaris* reference sequence (*Phaseolus vulgaris* v2.1, DOE-JGI and USDA-NIFA, http://phytozome.jgi.doe.gov/) using Strand NGS software version 2.0 (San Francisco, CA). The sequence alignment/map (SAM) files were used for further analysis. Quality control was assessed by the Strand NGS program, which determined the pre- and post-alignment quality of the reads for each sample. The aligned reads were then filtered based on alignment score, match count, mapping quality, and average base quality. After filtering, the aligned reads were normalized and quantified using the differential expression sequences (DEseq) algorithm and the Strand NGS program. Fold change (≥ 2) was determined for each sample by the Strand

NGS software based on the normalized data. Gene ontology (GO) analysis was performed on genes that were either upregulated or downregulated for each condition using AgriGO [54] (S1 Fig) and the Classification Super Viewer Tool at BAR (http://bar.utoronto.ca).

Hierarchical clustering was performed according to Eisen et al. [55], and the results were visualized with TreeView. Graph-based visualization of GO categories and interactive graphs were developed by REVIGO [56]. The pathway networks were obtained from KEGG Plant (http://www.kegg.jp/kegg/genome/plant.html) [57]. Heat maps were drawn with fold-change values using the R package (https://www.r-project.org/). Venn diagrams were constructed with DEG numbers using Lucidchart software (https://www.lucidchart.com/).

Results

Establishment of *P. vulgaris* root symbiosis with AMF and rhizobia

To elucidate the symbioses-root transcriptome datasets of *P. vulgaris*-AMF and *P. vulgaris*-rhizobia, root tissues individually colonized either with *R. irregularis* or *R. tropici* were established. Initially, the colonization kinetics of mycorrhized roots were assessed at three different time points. At 1 week post inoculation (wpi), the mycorrhized wild-type roots contained all relevant fungal structures, including hyphopodia, extraradical hyphae, intraradical hyphae, vesicles, developing (immature) arbuscules, and mature arbuscules. However, at 2 and 3 wpi, the %RLC of total vesicles and arbuscules displayed a >1-fold increase compared with those at 1 wpi (Fig 1A). RT-qPCR analysis was performed for PvPT4 (*P. vulgaris PHOSPHATE TRANSPORTER 4*) and PvNIN (*P. vulagris NODULE INSEPTION*) to rule out cross contamination of the symbionts due to their specific induction only in presence of mycorrhiza or rhizobia, respectively. RT-qPCR analysis revealed that higher levels (>2-fold) of AMF induced PvPT4 transcript accumulation at 2 wpi, and the same expression levels were maintained at 3 wpi in mycorrhized roots (Fig 1B). Subsequent analysis confirmed that these mycorrhized root samples lacked nodules and rhizobial symbiosis-specific PvNIN transcript, indicating that the samples were free of rhizobial cross-contamination (Figs 1E and 1F). The uninoculated control (henceforth designated as control) root tissues lacked AMF fungal structures at all observed time points (Fig 1A). The total P concentrations were significantly higher in leaves of mycorrhized plants than in control leaves (Fig 1C). Among the leaves of mycorrhized plants P concentrations were found to be increase over one-fold in 2 and 3 wpi samples compared with that at 1 wpi (Fig 1C).

Rhizobial colonization was assessed at three stages (1, 2, and 3 wpi). Similar to mycorrhized roots, rhizobial-inoculated roots display a >3-fold increase in nodule density at 2 and 3 wpi compared with those at 1 wpi. However, roots at 2 wpi lacked senesced nodules and fixed more atmospheric nitrogen than did roots at 1 and 3 wpi (Fig 1E and 1G). Nodulation-specific PvNIN transcript expression was observed only in rhizobial-inoculated roots (Fig 1F). Subsequent analysis confirmed that these nodulated root samples lacked AMF symbiosis-specific PvPT4 transcript expression, and the %RLC was zero, indicating that the samples were free of AMF cross-contamination (Fig 1A and 1B). Control roots also were free of rhizobial contamination (Fig 1E and 1G). These combined results indicate that 2 wpi *P. vulgaris* root tissues inoculated with either *R. irregularis* (Fig 1D) or *R. tropici* (Fig 1H) were ideal for further analysis because they had active P uptake (determined by PvPT4 expression and total leaf P concentrations) and active biological nitrogen fixation.

Transcriptome profiling and DEGs of *P. vulgaris* roots during symbiotic colonization

To better understand the molecular landscape of *P. vulgaris* genes that respond during colonization of two divergent root symbionts, we performed genome-wide expression profiling of
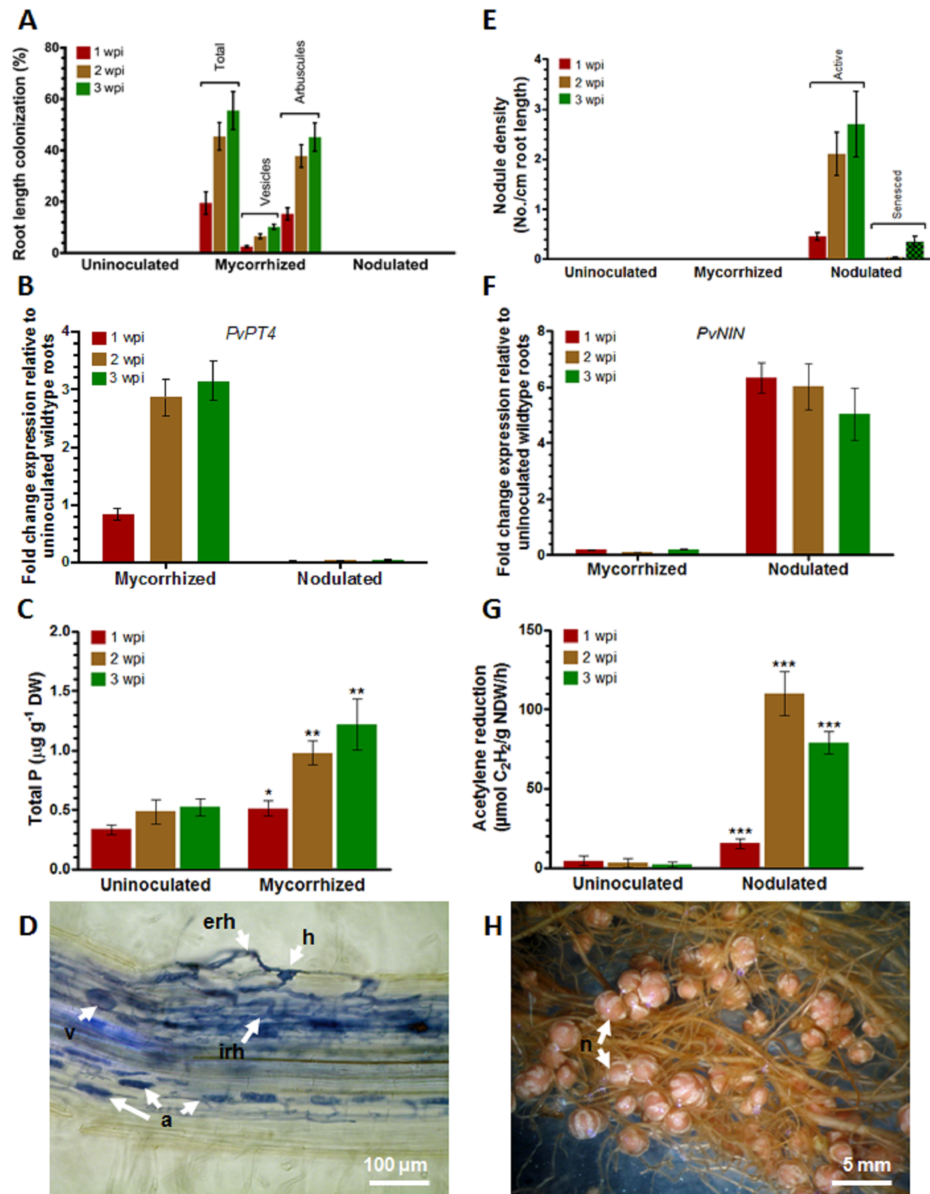
Fig 1. Determination of mycorrhizal and rhizobial colonization in *P. vulgaris* roots. Control (uninoculated), mycorrhized (*R. irregularis*), and nodulated (*R. tropici*) root samples were assessed at different time points for symbiotic colonization. (A) Percent mycorrhizal root length colonization. (B) RT-qPCR analysis of mycorrhizal-induced PvPT4 transcript levels. (C) Total shoot phosphorus concentration. (D) Representative image showing fungal structures in trypan blue-stained roots at 2 weeks post inoculation (wpi) with *R. irregularis*. (E) Nodule density. (F) RT-qPCR analysis of rhizobial-induced PvNIN transcript levels. (G) Nitrogen-fixing activity measured by acetylene reduction assay. (H) Representative image showing root nodules at 2 wpi with *R. tropici*. erh, extraradical hyphae; h, hyphopodia; irh, intraradical hyphae; v, vesicle; a, arbuscule; n, nodule. Error bars on the graphs represent mean ± SD of three biological replicates (n = 9). Statistically significant differences are indicated by asterisks (unpaired two-tailed Student's *t* test; *$P<0.05$, **$P<0.01$, ***$P<0.001$).

https://doi.org/10.1371/journal.pone.0182328.g001

mRNA from control and 2 wpi mycorrhized and nodulated roots using Ion Proton sequencing (S2 Table). Hierarchical cluster-derived control, mycorrhized, and nodulated dendrograms revealed that the transcript expression levels from two independent (biological) replicates of each group clustered together (S2 Fig). These data were then deposited in the National Center

for Biotechnology Information (NCBI) with accession number of PRJNA388751 (https://
www.ncbi.nlm.nih.gov/bioproject/388751). Based on statistical analysis of expression levels
(unpaired Student´s t-test, P-values of ≤ 0.05 and fold-change cut-off for upregulation and
downregulation of ≥2.0; S3 Table), we identified 1,959 upregulated and 1,260 downregulated
P. vulgaris DEGs during mycorrhizal colonization (Fig 2A and 2B). During nodulation, we
identified 1,247 upregulated and 1,398 downregulated DEGs (Fig 2A and 2C). Venn diagrams
illustrate the presence of shared DEGs between the two symbiont–plant interactions (Fig 2D).
Our analysis revealed that 288 of the total upregulated genes (14.7 and 23% of upregulated
genes in mycorrhized and nodulated roots, respectively) and 223 of the total downregulated
genes (17.7 and 16% of downregulated genes in mycorrhized and nodulated roots, respec-
tively) overlapped between these symbiotic conditions. The overlapping DEGs clustered into
four comparison groups, revealing that 106 genes specifically upregulated during mycorrhiza-
tion intersect with DEGs that were downregulated during nodulation. Conversely, 61 DEGs
that were upregulated during nodulation intersected with DEGs that were downregulated dur-
ing mycorrhization (Fig 2E).

A total of 1,959 upregulated and 1,260 downregulated mycorrhized DEGs and 1,247 upre-
gulated and 1,398 downregulated nodulated DEGs were assigned to three GO categories,
including biological process, molecular function, and cellular component. In the upregulated
DEGs of mycorrhized root samples, most of the 47% GO annotations belonged to BP, followed
by 39% GO annotations in MF and 14% in CC. In the downregulated mycorrhized root sam-
ples 46% belonged to BP, 34% in MF and 20% in CC. Similarly, the total number of GO terms
for upregulated nodulated root samples was 35% in BP, 35% in MF, and 30% in CC; in down-
regulated DEGs of nodulated roots show 46% GO annotations in BP, 34% in MF and 20% in
CC (S4 Table). The BP category from both mycorrhized and nodulated roots contained high
percent frequency of protein metabolism processes, energy pathways, other metabolic pro-
cesses, signal transduction, transport and response to stress (Fig 3); minor groups within this
category included immune system process, peptide transport, defense response, response to
oxidative stress, and cell wall macromolecule catabolism (S4 Table). The most abundant
groups in the molecular function category were binding, catalytic activity, hydrolase activity,
oxidoreductase activity, kinase (protein) activity, and transferase activity. Minor sub-groups in
the molecular function category included transmembrane/transporter activity, transcription
factors, peroxidase activity, heme binding, and antioxidant activity. In the CC category most
abundant groups were cell wall and plasma membrane in both mycorrhized and nodulated
samples. In general, the GO terms remain largely same in all the three categories however, the
percent frequency of these GO terms were varied among them (Fig 3A–3D). Next, we used
REVIGO to develop a graph-based visualization tool for the biological process and molecular
function GO categories (S3 Fig). In mycorrhized root samples, metabolism (phosphorus
metabolism, phosphate/nitrogen-containing compound metabolism, glucan metabolism),
membrane transport, peroxidase activity, cell wall, oxido-reduction processes and defense-
related GO terms were linked together (S3A and S3B Fig). In nodulated root samples, GO
terms related to transmembrane transport, binding, peroxidase activity, cell wall, defense, and
oxido-reduction processes were linked together (S3C and S3D Fig). The results obtained from
GO functional annotations and interactive graphs of the DEGs suggest that several major and
minor groups of all three GO categories were present at different percentages in both mycor-
rhized and nodulated roots of P. vulgaris (Fig 3; S6 Table).

To validate the RNA-Seq results, 12 DEGs with different expression patterns were selected
for RT-qPCR analysis (S1 Table) and then compared these results with the transcriptomic data
obtained through RNA-Seq. AMF induces the expression of the GRAS-domain transcription
factor RAM1 [17], and RAM1 induces RAM2, which produces cutin monomers during
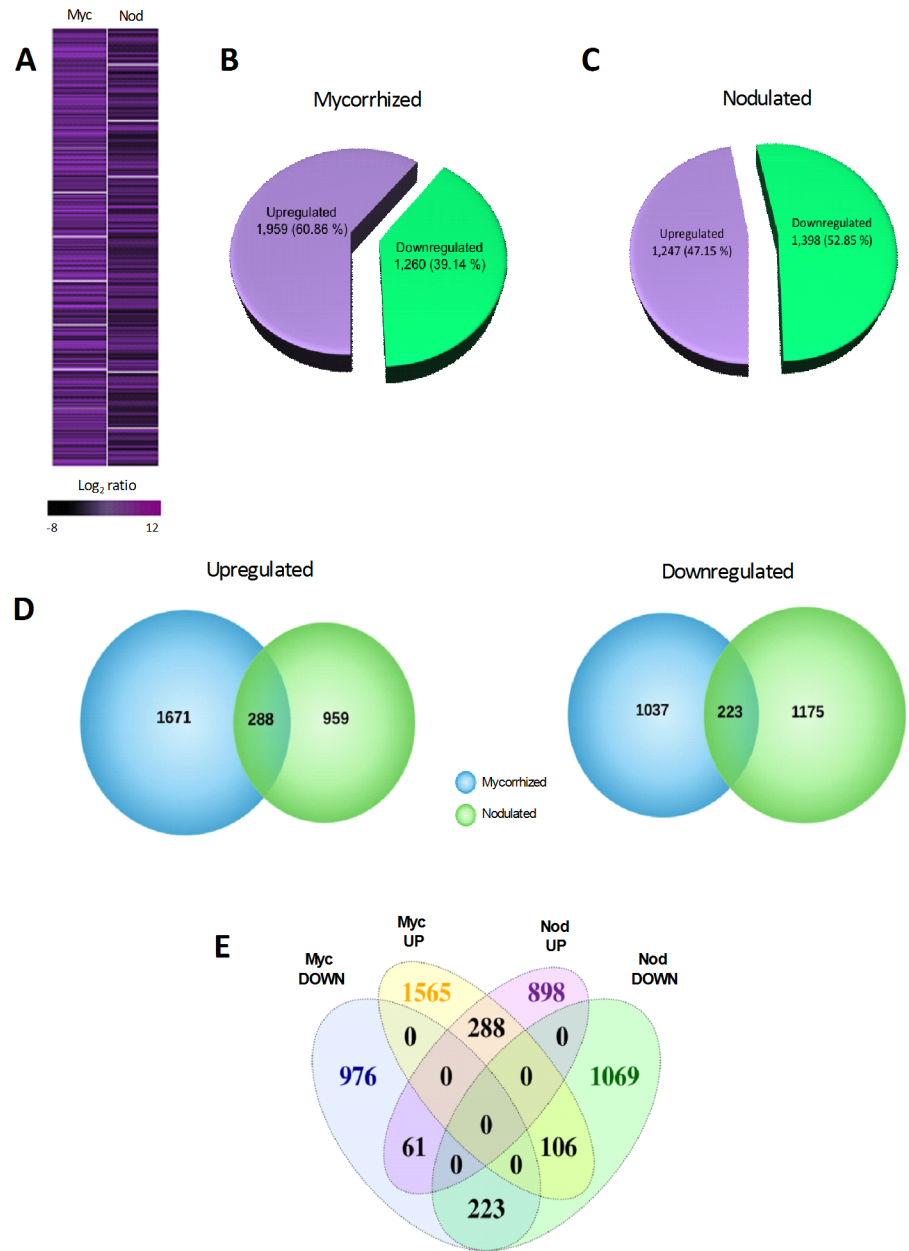
Fig 2. Summary of genome-wide expression profiling and identified DEGs in response to mycorrhizal and rhizobial colonization in *P. vulgaris* roots. Global transcriptome profile of genes upregulated and downregulated in response to arbuscular mycorrhizal fungi and rhizobia (unpaired Student´s *t*-test, *P*-values of ≤0.05 and fold-change of ≥2.0 upregulated and downregulated) (A). Number and percent distribution of uniquely expressed upregulated and downregulated genes during (B) mycorrhizal and (C) nodulation conditions. The *P. vulgaris* locus names and descriptions are listed in S3 Table. Venn diagram showing (D) shared DEGs (left side, upregulated genes; right side, downregulated genes) and (E) number of overlapping DEGs in upregulated and downregulated mycorrhized and nodulated roots (clustered into four comparison groups represented by four ellipses).

appressorium formation [18]. Infection and nodulation induces the expression of ERN1 (ETHYLENE-RESPONSIVE BINDING DOMAIN FACTOR REQUIRED FOR NODULA-TION) [58] and EARLY NODULATION 40 (ENOD40) [12]. We obtained similar results
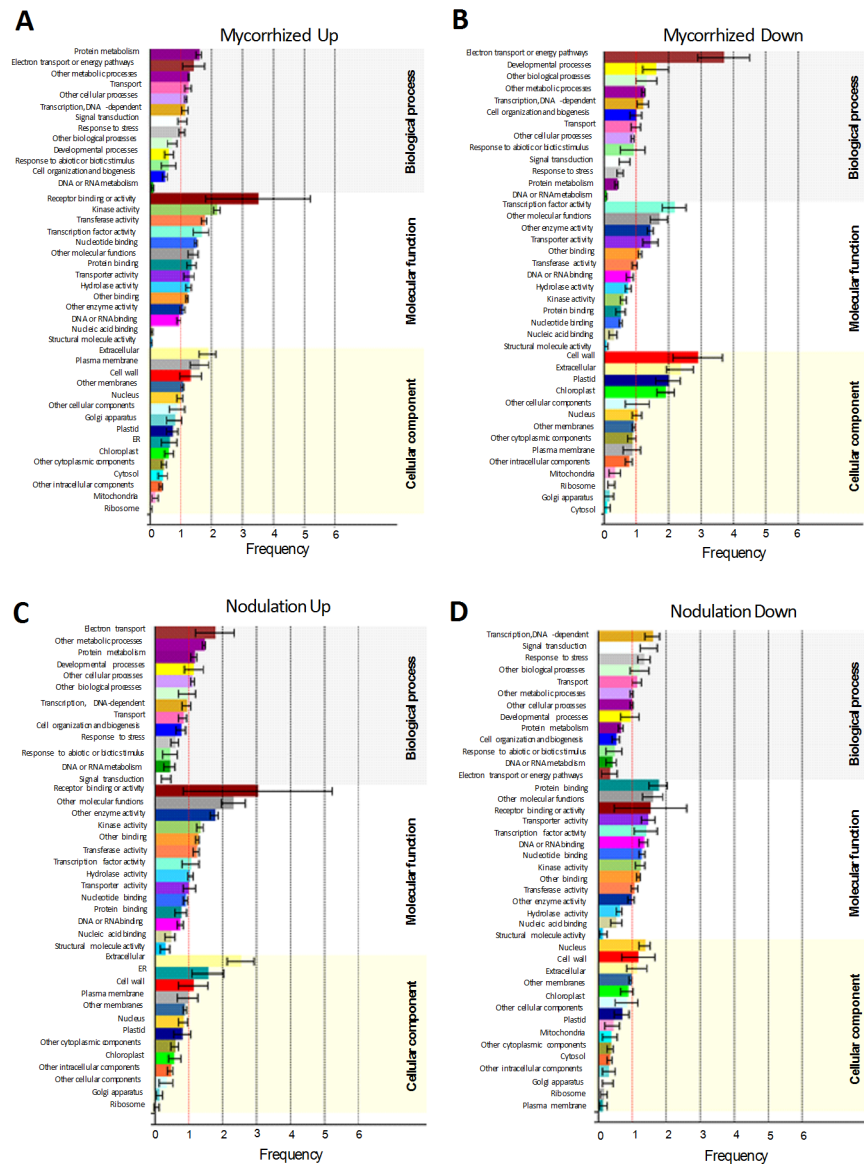
Fig 3. Gene ontology (GO) annotations of differentially expressed genes (DEG) in symbiont-colonized *P. vulgaris* roots. GO term annotation of (A) upregulated and (B) downregulated DEGs in mycorrhized roots. GO term annotation of (C) upregulated and (D) downregulated DEGs in nodulated roots. The DEGs were summarized in three main GO categories, biological process, molecular function and cellular component. The analysis was performed using classification Super Viewer tool at The Bio-Analytic Resource (BAR) for Plant Biology (http://bar.utoronto.ca) and the values of normed frequency was used to plot the graphs. The y-axis indicates the sub-categories and the x-axis indicates the frequency of a sub-category of genes in that category.

from both RT-qPCR and RNA-Seq analyses. RAM1 and RAM2 transcript levels were significantly increased in mycorrhized roots (Fig 4A), and ERN1 and ENOD40 transcripts were specifically induced in nodulated roots (Fig 4B). Further, ALC-INTERACTING 1 and AGAMO US-LIKE 8 were found to be upregulated whereas; HEMOPEXIN and SULFITE EXPORTER TAU-E were downregulated under mycorrhization (Fig 4A). Similarly, HAEMOGLOBIN 2 and SPERMIDINE HOC were upregulated and C2H2 ZINC FINGER LIKE and MATE
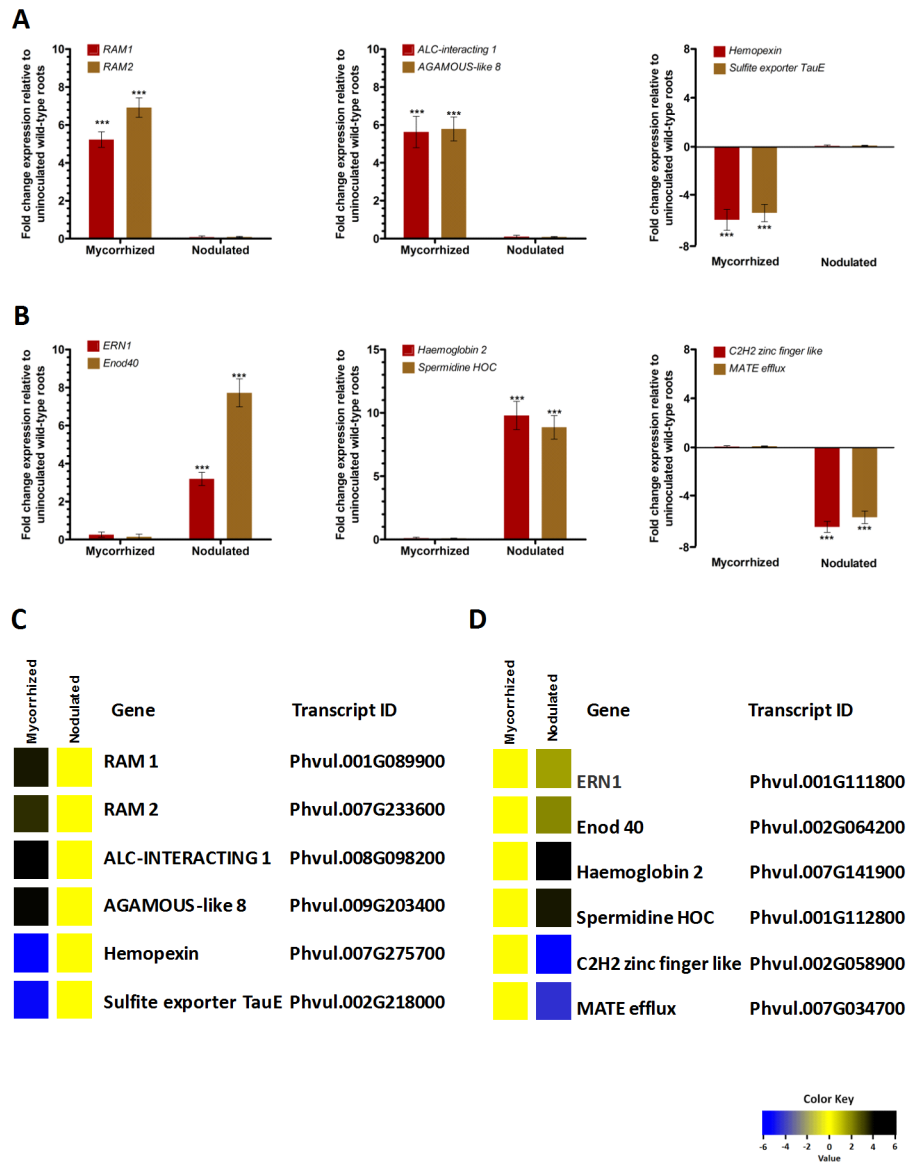
Fig 4. Validation of expression patterns of 12 DEGs of symbiont-colonized *P. vulgaris* roots by RT-qPCR analysis. Twelve DEGs (differentially expressed genes) showed similar expression patterns between RT-qPCR data (A and B) and RNA-Seq data (C and D). These genes included four genes well characterized mycorrhizal symbiosis specific RAM1 and RAM2, nodule specific ERN1 and ENOD40; Four genes ALC-INTERACTING 1, AGAMOUS-LIKE 8 and HEMOPEXIN, SULFITE EXPORTER TAU-E that are up- and down-regulated under mycorrhization, respectively; two genes HAEMOGLOBIN 2, SPERMIDINE HOC and C2H2 ZINC FINGER LIKE, MATE EFFLUX up- and down-regulated under nodulation, respectively. RT-qPCR data are the averages of three biological replicates (*n*>9). Statistical significance of differences between mycorrhized and nodulated roots was determined using an unpaired two-tailed Student's *t*-test (***P<0.001). Error bars represent means ± SEM.

EFFLUX downregulated under nodulation conditions (Fig 4B). These results were consistent with those observed in RNA-Seq data of mycorrhized roots (Fig 4C) and nodulated roots (Fig 4D). Thus, the RNA-Seq results were considerably reliable for the identification of DEGs during mycorrhizal or rhizobial colonization in this study.

Comparison of gene expression profiles in roots colonized by AMF and rhizobia

Defense-responsive genes.   Plants mobilize strong defense responses to effectively ward off pathogens [59]. Plants also engage in symbiotic relationships with advantageous microorganisms such as root-associated bacteria or fungi, which enhance nutrient resources for plants [60,47]. These symbiotic relationships become established by the induction or suppression of mechanisms associated with plant defense. To elucidate changes in host plant defenses induced by AMF or nodule symbioses, we assessed DEGs in mycorrhized and nodulated roots using AgriGO and REVIGO. Based on GO analysis we observed a total of 35 and 28 differentially responding defense genes in mycorrhized and nodulated roots, respectively. The Venn diagram intersection revealed 51 unique (29 in AMF and 22 in rhizobial symbioses) and 6 overlapping defense genes in the colonized roots (Fig 5A). Among the unique genes, 28 were upregulated and 1 was downregulated in mycorrhized roots, whereas 3 were upregulated and 19 were downregulated in nodulated roots (S4A and S5 Figs and S6 Table). Interestingly, 23 unique genes of mycorrhized roots and 16 unique genes of nodulated roots belonging to disease resistance protein family (TIR-NBS-LRR class) were found upregulated and downregulated, respectively. Similarly, two unique genes of MLP-like protein family members were upregulated while mycorrhization and downregulated during nodulation (S5 Fig, S5 Table). Among the overlapping genes, one TIR-NSB-LRR family member (Phvul.010G028700) and one BET V I family member (Phvul.011G183900) were upregulated during mycorrhizal colonization and downregulated during rhizobial colonization (Fig 5B). The observation that these two genes have opposite expression patterns during the two symbioses suggests that these genes could act as defense markers during symbiotic interactions. We also analyzed the known genes associated with *P. vulgaris* defense from the jasmonic acid (JA) and salicylic acid (SA) KEGG signaling pathways (plant signal transduction). The JASMONATE ZIM-DOMAIN (JAZ) genes are important repressors of the JA signaling pathway [61]; they were upregulated during mycorrhization and were variably expressed (i.e., exhibited both upregulation and downregulation of different transcripts of the same gene) during nodulation. The expression of JASMONATE RESISTANCE (JAR1), a pathogen defense gene [62], was downregulated during mycorrhizal colonization and upregulated during nodulation (S6 Fig; S6 Table). NPR1 was variably expressed in AMF-colonized roots and upregulated in nodulated roots compared with controls. Downstream genes such as TGA and PR-1 were variably expressed during both types of symbioses, except PR-1 was suppressed during mycorrhizal colonization compared with the control (S6 Fig; S6 Table). These results suggest that different isoforms of defense genes are elicited in *P. vulgaris* roots during AMF and rhizobial symbioses.

Cell wall-related genes.   The plant cell wall acts as a physical barrier against invading pathogens and parasites [63]. By contrast, the cell wall is modified during penetration and establishment of the symbiotic interface in AMF and rhizobial symbioses [64]. In the present study, based on GO analysis we observed 37 and 18 cell wall-related genes that were differentially regulated (upregulation and downregulation fold-change of ≥2.0) in *P. vulgaris* roots during AMF and rhizobial symbioses, respectively. A total of 21 genes were upregulated and 15 were downregulated in AMF-colonized roots, whereas 12 were upregulated and 5 were downregulated during nodulation (S4B and S7 Figs). The Venn diagram intersection identified 9 overlapping genes, 28 unique genes during mycorrhizal colonization, and 9 unique genes during nodulation (Fig 5C). These belong to different enzyme isoforms that target the plant cell wall by wall-loosening activities, including PECTIN-RELATED genes, PLANT INVERTASE and XYLOGLUCAN ENDOTRANSGLUCOSYLASE/HYDROLASE (XTH). On the other hand, expansin proteins non-enzymatically trigger a pH dependent relaxation of the
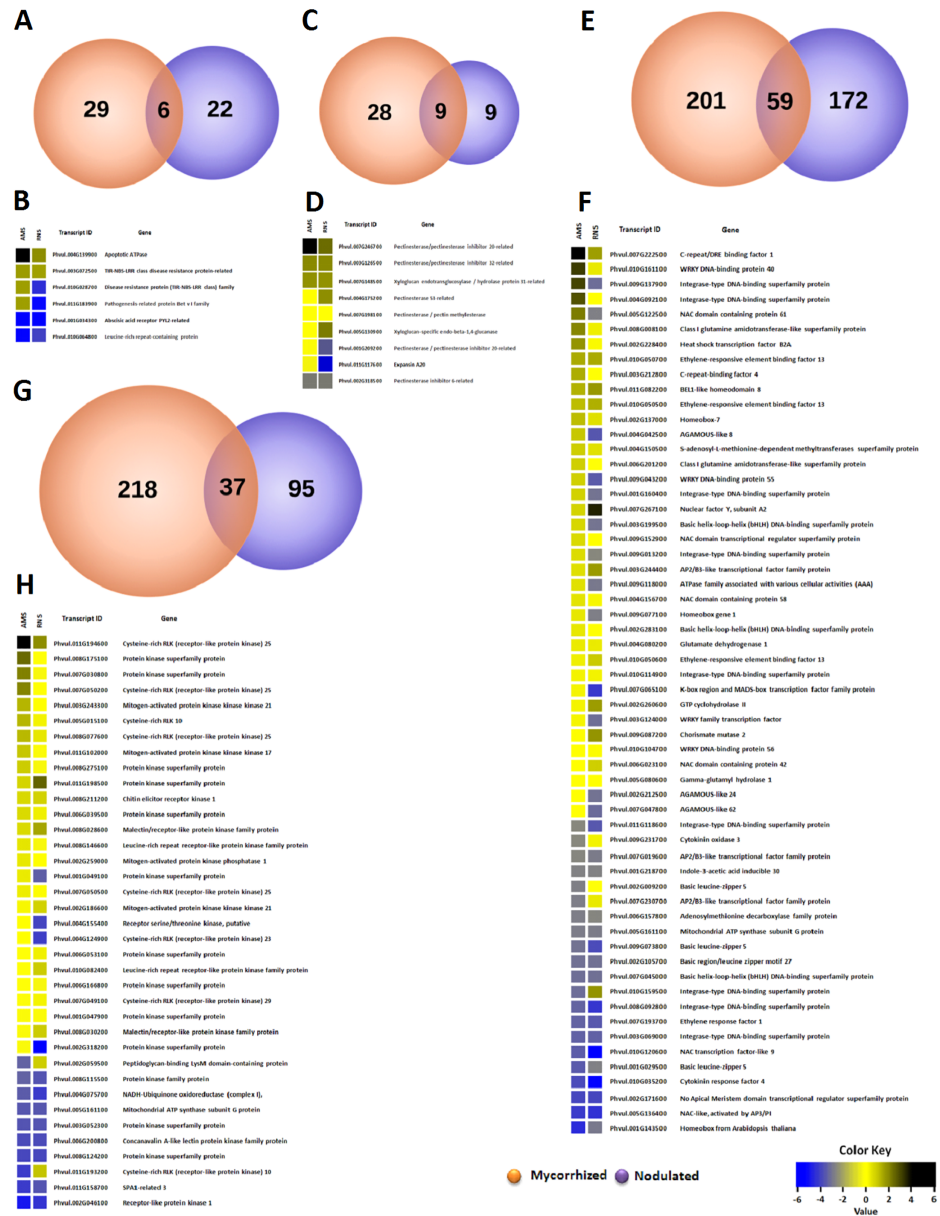
A 29 | 6 | 22

C 28 | 9 | 9

E 201 | 59 | 172

B

		Transcript ID	Gene
		Phvul.004G199900	Apoptotic ATPase
		Phvul.003G072500	TIR-NBS-LRR class disease resistance protein-related
		Phvul.010G028700	Disease resistance protein (TIR-NBS-LRR class) family
		Phvul.011G183900	Pathogenesis-related protein Bet v I family
		Phvul.001G044600	Abscisic acid receptor PYL2-related
		Phvul.010G064800	Leucine-rich repeat-containing protein

D

		Transcript ID	Gene
		Phvul.005G266700	Pectinesterase/pectinesterase inhibitor 20-related
		Phvul.009G126500	Pectinesterase/pectinesterase inhibitor 12-related
		Phvul.001G148500	Xyloglucan endotransglucosylase / hydrolase protein 31-related
		Phvul.004G175200	Pectinesterase 53-related
		Phvul.001G198100	Pectinesterase / pectin methylesterase
		Phvul.005G130900	Xyloglucan-specific endo-beta-1,4-glucanase
		Phvul.005G309200	Pectinesterase / pectinesterase inhibitor 20-related
		Phvul.015G176500	Expansin A20
		Phvul.001G313500	Pectinesterase inhibitor 6-related

G 218 | 37 | 95

F

		Transcript ID	Gene
		Phvul.007G222500	C-repeat/DRE binding factor 1
		Phvul.010G161100	WRKY DNA-binding protein 40
		Phvul.009G137900	Integrase-type DNA-binding superfamily protein
		Phvul.004G092100	Integrase-type DNA-binding superfamily protein
		Phvul.005G122500	NAC domain containing protein 61
		Phvul.008G008100	Class I glutamine amidotransferase-like superfamily protein
		Phvul.022G228400	Heat shock transcription factor B2A
		Phvul.010G050700	Ethylene-responsive element binding factor 13
		Phvul.003G212800	C-repeat-binding factor 4
		Phvul.011G082200	BEL1-like homeodomain 8
		Phvul.010G050500	Ethylene-responsive element binding factor 13
		Phvul.002G137000	Homeobox-7
		Phvul.004G042500	AGAMOUS-like 8
		Phvul.004G150500	S-adenosyl-L-methionine-dependent methyltransferases superfamily protein
		Phvul.006G201200	Class I glutamine amidotransferase-like superfamily protein
		Phvul.009G043200	WRKY DNA-binding protein 55
		Phvul.016160400	Integrase-type DNA-binding superfamily protein
		Phvul.007G267100	Nuclear factor Y, subunit A2
		Phvul.003G199500	Basic helix-loop-helix (bHLH) DNA-binding superfamily protein
		Phvul.009G152900	NAC domain transcriptional regulator superfamily protein
		Phvul.009G013200	Integrase-type DNA-binding superfamily protein
		Phvul.003G244400	AP2/B3-like transcriptional factor family protein
		Phvul.009G118000	ATPase family associated with various cellular activities (AAA)
		Phvul.004G156700	NAC domain containing protein 58
		Phvul.009G071100	Homeobox gene 1
		Phvul.002G283100	Basic helix-loop-helix (bHLH) DNA-binding superfamily protein
		Phvul.004G080200	Glutamate dehydrogenase 1
		Phvul.010G050600	Ethylene-responsive element binding factor 13
		Phvul.010G114900	Integrase-type DNA-binding superfamily protein
		Phvul.007G065100	K-box region and MADS-box transcription factor family protein
		Phvul.002G260600	GTP cyclohydrolase II
		Phvul.001G324000	WRKY family transcription factor
		Phvul.009G087200	Chorismate mutase 2
		Phvul.010G104700	WRKY DNA-binding protein 56
		Phvul.006G023100	NAC domain containing protein 42
		Phvul.005G080600	Gamma-glutamyl hydrolase 1
		Phvul.002G212500	AGAMOUS-like 24
		Phvul.007G047800	AGAMOUS-like 62
		Phvul.011G118600	Integrase-type DNA-binding superfamily protein
		Phvul.009G231700	Cytokinin oxidase 3
		Phvul.007G019600	AP2/B3-like transcriptional factor family protein
		Phvul.001G218700	Indole-3-acetic acid inducible 30
		Phvul.002G009200	Basic leucine-zipper 5
		Phvul.007G210700	AP2/B3-like transcriptional factor family protein
		Phvul.006G157800	Adenosylmethionine decarboxylase family protein
		Phvul.005G161100	Mitochondrial ATP synthase subunit G protein
		Phvul.009G073800	Basic leucine-zipper 5
		Phvul.002G105700	Basic region/leucine zipper motif 27
		Phvul.007G045000	Basic helix-loop-helix (bHLH) DNA-binding superfamily protein
		Phvul.010G159500	Integrase-type DNA-binding superfamily protein
		Phvul.008G092800	Integrase-type DNA-binding superfamily protein
		Phvul.007G193700	Ethylene response factor 1
		Phvul.003G069000	Integrase-type DNA-binding superfamily protein
		Phvul.010G120600	NAC transcription factor-like 9
		Phvul.001G029500	Basic leucine-zipper 5
		Phvul.010G039200	Cytokinin response factor 4
		Phvul.002G371600	No Apical Meristem domain transcriptional regulator superfamily protein
		Phvul.005G316400	NAC-like, activated by AP3/PI
		Phvul.001G143500	Homeobox from Arabidopsis thaliana

H

		Transcript ID	Gene
		Phvul.011G194600	Cysteine-rich RLK (receptor-like protein kinase) 25
		Phvul.008G175100	Protein kinase superfamily protein
		Phvul.007G030800	Protein kinase superfamily protein
		Phvul.007G050200	Cysteine-rich RLK (receptor-like protein kinase) 25
		Phvul.009G243300	Mitogen-activated protein kinase kinase kinase 21
		Phvul.005G015100	Cysteine-rich RLK 10
		Phvul.008G077600	Cysteine-rich RLK (receptor-like protein kinase) 25
		Phvul.011G102000	Mitogen-activated protein kinase kinase kinase 17
		Phvul.009G275100	Protein kinase superfamily protein
		Phvul.011G198500	Protein kinase superfamily protein
		Phvul.008G211200	Chitin elicitor receptor kinase 1
		Phvul.006G039500	Protein kinase superfamily protein
		Phvul.008G028600	Malectin/receptor-like protein kinase family protein
		Phvul.008G146600	Leucine-rich repeat receptor-like protein kinase family protein
		Phvul.002G259000	Mitogen-activated protein kinase phosphatase 1
		Phvul.001G049100	Protein kinase superfamily protein
		Phvul.007G050500	Cysteine-rich RLK (receptor-like protein kinase) 25
		Phvul.002G186600	Mitogen-activated protein kinase kinase kinase 21
		Phvul.004G155400	Receptor serine/threonine kinase, putative
		Phvul.004G124900	Cysteine-rich RLK (receptor-like protein kinase) 23
		Phvul.006G053100	Protein kinase superfamily protein
		Phvul.010G082400	Leucine-rich repeat receptor-like protein kinase family protein
		Phvul.004G166800	Protein kinase superfamily protein
		Phvul.007G049100	Cysteine-rich RLK (receptor-like protein kinase) 29
		Phvul.001G047900	Protein kinase superfamily protein
		Phvul.008G030200	Malectin/receptor-like protein kinase family protein
		Phvul.005G318200	Protein kinase superfamily protein
		Phvul.002G059500	Peptidoglycan-binding LysM domain-containing protein
		Phvul.008G115500	Protein kinase family protein
		Phvul.004G075700	NADH-Ubiquinone oxidoreductase (complex I),
		Phvul.005G161100	Mitochondrial ATP synthase subunit G protein
		Phvul.005G052300	Protein kinase superfamily protein
		Phvul.006G200800	Concanavalin A-like lectin protein kinase family protein
		Phvul.008G124200	Protein kinase superfamily protein
		Phvul.011G193200	Cysteine-rich RLK (receptor-like protein kinase) 10
		Phvul.001G158700	SPA3-related 3
		Phvul.002G046100	Receptor-like protein kinase 1

🟠 Mycorrhized 🟣 Nodulated

Color Key
-6 -4 -2 0 2 4 6
Value

Fig 5. RNA-Seq based transcriptome comparison of genes induced by AMF and rhizobia in *P. vulgaris* roots. Differentially expressed genes upregulated and downregulated in response to AMF and rhizobia in *P. vulgaris* roots were identified based on *P*-values of ≤0.05 and fold-change of ≥2.0 (upregulated and downregulated). Unique and shared genes were identified after a pairwise comparison between treatments. Venn diagrams representing the number of DEGs involved in processes related to (A) defense, (C) cell wall, (E) nitrogen metabolism, and (G) phosphate metabolism. Heat maps of the overlapping gene expression patterns during mycorrhizal and rhizobial colonization for processes related to (B) defense, (D) cell wall, (F) nitrogen metabolism, and (H) phosphate metabolism. Color bar shows the fold-change range, with red and green representing downregulation and upregulation, respectively.

https://doi.org/10.1371/journal.pone.0182328.g005

cell wall which loosens and softens during cell expansion. Among the overlapping genes, XYLOGLUCAN-SPECIFIC ENDO-BETA-1,4-GLUCANASE (Phvul.005G130900) and PEC-TINESTERASE 53-RELATED (Phvul.004G175200) genes were downregulated during mycorrhizal colonization and upregulated during nodulation. We observed that EXPANSIN A20

was downregulated under both symbiotic conditions (Fig 5D, S6 Table). Among the unique genes, EXPANSIN-LIKE A2 and EXPANSIN B3 were upregulated, whereas EXPANSIN A7 and EXPANSIN A18 were downregulated under mycorrhization; EXPANSIN A15, EXPANSIN-LIKE B1 and B2 were upregulated under nodulation (S7 Fig; S6 Table). We observed that EXPANSIN A20 was downregulated and EXPANSIN-LIKE B2 was upregulated under both symbiotic conditions (Fig 5D, S7 Fig). Ten and nine unique genes belonging to PLANT INVERTASE/PECTIN METHYLESTERASE INHIBITOR superfamily and XTH family are the most abundant class of enzymes found in mycorrhized roots, respectively. Among the unique genes of nodulation, only two members for each of these enzymes were differentially expressed (S7 Fig; S6 Table). Pectin methylesterase is post-transcriptionally regulated by endogenous protein inhibitors and functions to maintain cell wall integrity in plant immunity whereas, xyloglucan endotransglucosylase enzyme cleaves and religates xyloglucan polymers and is an essential constituent of the primary cell wall in growing tissues [65,66]. These combined results indicate that several enzyme isoforms regulating cell wall remodeling in *P. vulgaris* are uniquely expressed during these symbioses, thereby modifying cell wall plasticity during plant–symbiont interactions.

Nitrogen compound metabolism. Nitrogen metabolism is an important pathway in plants, and it is specifically crucial for nodulating plants. We compared the expression of genes involved in N metabolism in *P. vulgaris* roots during AMF and rhizobial symbioses, and identified a total of 260 DEGs in AMF symbiosis and 231 DEGs in rhizobial symbiosis based on GO analysis. Of these, 173 genes were upregulated and 87 were downregulated in mycorrhization, whereas 112 genes were upregulated and 119 were downregulated during nodulation (S4C and S8 Figs). We identified 59 overlapping genes involved in N metabolism in the two symbiotic interactions (Fig 5E); of these, 38 and 29 genes were upregulated and 21 and 30 were downregulated during AMF and rhizobial symbioses, respectively (Fig 5F).

Recent work demonstrated that the AP2 transcription factor is a key player in soybean nodule initiation [67]. Nodule initiation and differentiation are controlled by the ETHYLENE-RESPONSIVE TRANSCRIPTION FACTOR 1 (ERF1 [68]) in *L. japonicus* and the EDF [69] and MADS-BOX transcription factors NGL9 and NMH7 [70] in *Medicago* species. A recent study by Azarakhsh et al. [71] reported that a homeobox transcription factor (KNOTTED1-LIKE) regulates cytokinin biosynthesis during nodule development in *M. truncatula*. However, little is known about the role of these genes during AMF symbiosis. In this study, we found that most of the N metabolism genes belong to different transcription factor families (Fig 5F, S8 Fig). Unique genes and different homologs of the AP2 DOMAIN, ERF, MADS-BOX genes, and HOMEOBOX transcription factors (S5 Table) were differentially expressed in *P. vulgaris* roots during AMF and rhizobial symbioses (S8 Fig). Among the overlapping genes, the AP2/B3 TFs such as Phvul.003G244400 is upregulated, Phvul.007G019600 is downregulated in both symbioses. Whereas Phvul.007G230700 (AP2/B3 TF) is downregulated during mychorrhiza colonization and Phvul.007G065100 (MADS-BOX) is downregulated during rhizobia colonization (Fig 5F; S6 Table), indicating that gene expression in the host root is differentially elicited depending on the type of symbiosis. During nitrogen fixation in tropical legumes like bean, the ammonia is reduced in uninfected cells via purine oxidation to the ureides allantoin and allantoate [72]. These ureides are the main forms of organic nitrogen transported and stored in plants [73]. As anticipated, genes involved in purine biosynthesis (PHOSPHORIBOSYL PYROPHOSPHATE AMIDOTRANSFERASE, GLYCINE LIGASE, and PHOSPHORIBOSYL AMINOIMIDAZOLE CARBOXYLASE), ureide biosynthesis (URICASE, XANTHINE DEHYDROGENASE 1, and ALLANTOINASE), and ammonia assimilation [GLUTAMINE SYNTHETASE and NADH-DEPENDENT GLUTAMATE SYNTHASE 2 (GOGAT)] were upregulated only in nodulated roots (S3 Table and S8 Fig). We also analyzed the gene

expression levels of all known key enzymes (15 genes) in the *P. vulgaris* KEGG nitrogen metabolism pathway. During mycorrhizal symbiosis, 8 of 15 gene transcripts were upregulated, 4 were downregulated, and 3 exhibited variable expression (S9A Fig; S6 Table). During rhizobial symbiosis, 12 of 15 genes were upregulated and 3 exhibited variable expression (S9B Fig; S6 Table). These gene profiles reflect different transcript abundance levels during the *P. vulgaris* response to AMF and rhizobia. The key genes and enzymes identified in the KEGG nitrogen metabolism pathway are strongly induced in response to rhizobial colonization, which primarily involves biological nitrogen fixation.

Phosphorus metabolism. The macronutrient P is crucial for the biosynthesis of key cellular biomolecules, and plants cannot grow without a reliable P supply. Inorganic phosphate (P_i) is involved in controlling key enzyme reactions and regulating metabolic pathways [74]. AMF aid the host plant with P_i uptake. Therefore, we compared the expression of genes involved in P metabolism during mycorrhizal and rhizobial colonization. Based on GO analysis we observed a total of 255 and 132 DEGs involved in P metabolism in response to mycorrhizal and rhizobial colonization, respectively (Fig 5G). Of these, 203 genes were upregulated and 52 were downregulated during mycorrhizal colonization, whereas 62 genes were upregulated and 70 were downregulated during rhizobial colonization (S4D Fig). The Venn diagram intersection identified 37 overlapping genes (Fig 5H) and 218 and 95 unique genes, respectively, during mycorrhizal and rhizobial colonization (S10 Fig). Among the overlapping genes, WALL-ASSOCIATED RECEPTOR KINASE C-TERMINAL (Phvul.001G049100, Phvul.002G3182 00), SALT STRESS RESPONSE/ANTIFUNGAL (Phvul.004G124900), and GLYCEROPHOSPHODIESTER PHOSPHODIESTERASE (GDPD; Phvul.004G155400) were upregulated during mycorrhizal symbiosis and downregulated during rhizobial symbiosis (Fig 5H). Conversely, a NON-SPECIFIC SERINE/THREONINE PROTEIN KINASE (Phvul.002G059500) was upregulated during rhizobial symbiosis and downregulated during mycorrhizal symbiosis. Isoforms of LECTIN-LIKE genes were found to be the most abundant class of upregulated unique genes in mycorrhized roots (S10 Fig). Several studies reported that lectin genes are expressed in arbuscule-containing cells in *M. truncatula* [75–77].

Next, we assessed the expression of 23 known genes and enzymes identified in the *P. vulgaris* KEGG inositol phosphate (IP) metabolism pathway; these are involved in regulating many cellular functions such as cell growth, apoptosis, endocytosis, and cell differentiation [78]. The transcripts of INOSITOL-PENTAKISPHOSPHATE 2-KINASE (IPK1) (involved in phytate biosynthesis, a phosphorous reservoir [79]), 1D-MYO-INOSITOL-TRIPHOSPHATE 3-KINASE, INOSITOL-1,4,5-TRISPHOSPHATE 5-PHOSPHATASE, and MYOTUBULARIN ISOFORMS [80] were all upregulated in mycorrhized roots (S11A Fig; S6 Table) and downregulated during nodulation (S11B Fig; S6 Table). The transcripts of INOSITOL-POLYPHOSPHATE MULTIKINASE family genes were downregulated in mycorrhized roots and upregulated during nodulation. These results confirm that most genes involved in P and IP metabolism are upregulated in *P. vulgaris* roots in response to mycorrhizal symbiosis, conditions that promote P uptake, compared with rhizobial symbiosis.

Discussion

Phaseolus vulgaris is one of the most extensively studied model legumes in the world. There has been a focus on gene functional characterization in recent years, specifically in the area of *Phaseolus*-rhizobia symbiosis [21,26–30]. However, studies on *Phaseolus*-AMF symbiosis are limited [33,81]. The availability of genetic resources such as expressed sequence tags [82] and global gene expression profiles [83] stimulated rapid advances in rhizobial symbiosis research. There are fewer resources for AMF symbiosis research in *Phaseolus*, and there is an urgent

need for their development. Some studies in other legumes have investigated symbiosis-induced responses in roots colonized by AMF and rhizobia using transcriptome data obtained from cDNA macroarrays and microarrays. Those studies selected samples for comparative transcriptomic analysis based on symbiotic structures in the roots of *L. japonicus* (27 dpi with AMF and 12 dpi with rhizobia [84]), *M. truncatula*, and *C. gluca* (45 dpi with AMF [37]). In the present study, systematic analyses were performed to identify an ideal symbiotic stage for investigating both mycorrhizal and rhizobial associations with wild-type *P. vulgaris* roots. At 2 wpi, mycorrhizal and rhizobial symbionts established mature symbiotic structures and were physiologically active in P uptake and N fixation, respectively. An RNA-Seq-based gene expression analysis in control, mycorrhized, and nodulated roots of *P. vulgaris* using Ion Proton sequencing provided a global gene expression profile under each condition. Statistics and observed expression levels were used to identify the DEGs (upregulated and downregulated) for mycorrhized and nodulated roots; subsequently, the data sets were compared. These combined analyses identified 3,219 DEGs (fold-change cut-off of ≥2.0 upregulated and downregulated) in response to mycorrhizal symbiosis and 2,645 in response to rhizobial symbiosis. RNA-Seq analyses identified a total of 3,641 DEGs during AMF development (27 dpi [84]) in *L. japonicus*, and 1,668 DEGs during nodulation (21 dpi) in *P. vulgaris* [83]. The RNA-Seq approach identified more DEGs than previous microarray studies in AMF- or arbuscule-containing cells [85–89], possibly because RNA-Seq provides more precise measurements of transcript levels and their isoforms, and it has a broader dynamic range than microarray methods [40]. The gene expression data obtained by our RNA-Seq analysis were validated for 12 DEGs with different expression patterns in *P. vulgaris* using RT-qPCR. Quantitative RT-PCR results were consistent with those observed in RNA-Seq data of mycorrhized and nodulated roots. For instance, the relative expression levels of the AMF-specific GRAS-domain transcription factor RAM1, RAM1-induced RAM2, and rhizobial-specific ERN1 and ENOD40 displayed similar fold-change expression trends using RNA-Seq. The same expression trends of RAM1, ERN1, and ENDO40 in *P. vulgaris* [32,34] and RAM2 in *M. truncatula* [18] were previously reported as symbiotic marker genes in legumes. The AgriGO platform was used to derive a total of 180 and 160 significant GO categories for mycorrhizal and rhizobial symbioses, respectively, including biological process, molecular function, and cellular component. Protein metabolism, other metabolic processes, transport, signal transduction, transcription factor activity, kinase activity, defense, cell wall and plasma membrane were few among the most abundant GO terms found in mycorrhizal and rhizobial symbioses samples. High similarity was identified previously in GO term enrichment data by Handa et al. [84] in mycorrhized roots of *L. japonicus* and *M. truncatula* roots treated with nod factor [90]. Our primary focus was to identify unique and shared genes involved in defense, cell wall-related processes, N metabolism, and P metabolism in mycorrhizal and rhizobial symbiosis.

To establish symbiotic interactions, host plants repress gene families involved in defense reactions. A previous transcriptome analysis using RNA-Seq in rhizobial-inoculated *M. truncatula* roots treated with the nitric oxide synthase inhibitor cPTIO [2-(4-CARBOXYPHENYL)-4,4,5,5-TETRAMETHYLIMIDAZOLINE-1-OXYL-3-OXIDE] detected downregulation of defense genes elicited by rhizobial inoculation [91]. Similarly, the expression profiles of arbuscule-containing cells indicated that some DEFENSIN and CHITINASE genes [87] are elicited, and some defense responses are suppressed [89,92]. Specific TIR-NBS-LRR proteins negatively regulate the jasmonic acid signalling genes [93], and such low JA signalling encourage AM fungal colonization in plants [94]. Herein, we found that TIR-NBS-LRR family genes were most abundant class of defence genes that differentially expressed in both symbioses. Interestingly, upregulation of 23 TIR-NBS-LRR members unique to mycorrhization could result in decreased expression of JAR1 which may be involved in suppression of defence against invading AM

fungi. Whereas, rhizobial colonization downregulated all the 16 unique TIR-NBS-LRR members therefore JAR1 expression was found upregulated which perhaps evoked the defence that might recognize the rhizobia as symbiont for successful colonization. Nevertheless, this hypothesis needs to be demonstrated. *Arabidopsis* JAR1 was upregulated in response to infection with the fungal pathogen *Botrytis cinerea* [95] and the bacterial pathogens *Pseudomonas syringae* and *Ralstonia solanacearum*, which activated the JA signaling pathway as a defense response [94]. In contrast to the response to the pathogenic fungus *B. cinerea*, we observed here that JAR1 expression was suppressed during mycorrhizal symbiosis. Although JAR1 is upregulated in nodulated roots, some PR-1 genes (salicylic acid-mediated defense) were variably expressed, indicating that rhizobial surface polysaccharides could suppress or help to evade this first basal defense [96,97]. Our combined results suggest that different defense gene isoforms (both unique and shared genes) exhibited differential responses to mycorrhizal and rhizobial symbioses.

Cell wall remodeling during root symbioses with microsymbionts facilitates the establishment of a close interface that enables developmental coordination and nutrient exchange. Cell wall remodeling accommodates plant cell growth, which begins with selective cell wall loosening, followed by water uptake and cell enlargement [98]. During mycorrhization and nodulation, several isoforms of cell wall-loosening genes such as PECTINS and XYLOGLUCAN ENDOTRANSGLUCOSYLASE/HYDROLASES were differentially expressed. Rich et al. [64] reported that symbiotic signals induced cell wall modifications during penetration and establishment of the symbiotic interface during nodulation and mycorrhization. In *Medicago* XYLOGLUCAN ENDOTRANSGLUCOSYLASE/HYDROLASES 1 (XTH1) promoter was highly active in mycorrhizal roots and its transcripts were significantly induced in upon mycorrhization [99]. Similarly, herein we observed XTH family proteins are one of the most abundantly expressing genes unique to mycorrhizal colonization suggesting its specificity to fungal symbiosis. A study in soybean shows that the root hair specific EXPANSIN B1 regulates formation of root hairs whereas; EXPANSIN B2 controls the root hair elongation [100]. Based on the fact that rhizobia invade the root via root hair cells [12] and interestingly in our study the unique genes of nodulated roots shows both EXPANSIN B1 and B2 transcripts were upregualted indicating its possible involvement in rhizbobial invasion into the host root. This notion was supported by a separate study where β-EXPANSIN gene expression profiles have been characterized during the early stage of mycorrhization and nodulation in *L. japonicus*, *Glycine max* (soybean), and *Melilotus officinalis* (sweet clover) [101]. Our study showed that unique EXPANSIN genes in *P. vulgaris* responded differentially to mycorrhizal and rhizobial symbioses. We also found that several unique cell wall-related genes involved in softening and remodeling the *P. vulgaris* root were differentially expressed during mycorrhizal and rhizobial symbioses.

Transcriptomic approaches provide powerful tools to investigate complex network interactions in N metabolism, which involves N uptake and regulation, amino acid metabolism, and N translocation and remobilization [102–104]. Several N metabolism genes that participate in rhizobial symbiosis have been characterized, such as MsNGL9 and MsNMH7 [70], LjERF1 [68], MtEDF [69], GmAP2 [67], and MtKNOTTED1-LIKE [71]. Genes encoding NF-Y subunits act as components of a hierarchical transcriptional activation cascade in the nodulation signaling pathway [21,25,104–106]. Reduction of PvNF-YC1 [25] and LjNF-YB [21] transcript levels by RNA interference leads to the arrest of nodule development and defective rhizobial infection. Genes involved in purine and ureide biosynthesis and ammonia assimilation have key roles in transport and storage of organic nitrogen in host plants [73]. Results from our present analysis support these observations, as bean homologs of these genes were upregulated during rhizobial symbiosis. We also obtained the expression profiles of N metabolism genes during mycorrhizal symbiosis. We observed that most genes involved in N metabolism in

mycorrhized roots belong to different transcription factor families; however, functional characterization studies are required to decipher their roles during AMF symbiosis.

In plants, depletion of P_i induces dramatic changes in developmental and metabolic programs and in transcriptomic, proteomic, and metabolomic profiles. AMF symbiosis can reduce the effects of P_i depletion in the rhizosphere, thereby improving plant P nutrition and growth [107]. The evolutionarily conserved P metabolism gene GDPD has an important role in several physiological processes in both prokaryotes and eukaryotes. *Arabidopsis* GDPD maintains cellular phosphate homeostasis under phosphate starvation [108]. We observed that GDPD was upregulated in mycorrhized *P. vulgaris* roots. AM-specific lectins are known to be incorporated into plant cell walls [77], and several isoforms of lectin-like proteins were induced in AMF-colonized roots. Some genes for lectin-like proteins were also upregulated during rhizobial symbiosis, although their functions have not been determined. Among the known genes and enzymes involved in the *P. vulgaris* inositol phosphate metabolism pathway, we observed that IPK1, 1D-MYO-INOSITOL-TRIPHOSPHATE 3-KINASE, INOSITOL-1,4,5-TRISPHOSPHATE 5-PHOSPHATASE, and different MYOTUBULARIN ISOFORMS were upregulated in AMF-colonized roots. IPK1 is implicated in the synthesis of phytate, a phosphate storage form that is used to maintain phosphate homeostasis in *Arabidopsis* [79]. Our combined data confirm that most genes involved in P and IP metabolism are upregulated in mycorrhized roots, which are primed to promote P uptake [74].

Conclusions

We performed comparative transcriptome analyses of *P. vulgaris* roots colonized by AMF and rhizobia, and identified differentially expressed unique and shared genes associated with defense, cell wall structure, N metabolism, and P metabolism. The identified DEGs may be involved in the formation of these beneficial symbiotic relationships. However, further research is required to determine the putative roles of these DEGs during specific symbiotic interactions. These investigations will extend our understanding of symbiotic genetic signaling networks, and identify candidate genes that could be targeted to enhance P uptake and N-fixing capacity, and thereby increase the net yield of this valuable grain legume.

Supporting information

S1 Fig. Overview of experimental design for RNA sequencing and data analysis.
(PDF)

S2 Fig. Heatmap showing hierarchical clustering based on expression values of transcripts in control, mycorrhized, and nodulated root samples.
(PDF)

S3 Fig. Interactive graph of biological processes and molecular function GO terms, as determined by AgriGO and REVIGO algorithms.
(PDF)

S4 Fig. Graphical representation of number of unique upregulated and downregulated genes that responded during mycorrhizal and rhizobial colonization.
(PDF)

S5 Fig. DEGs of defense-responsive genes during root symbioses.
(PDF)

S6 Fig. Effect of root symbiosis on plant signal transduction pathways in mycorrhized and nodulated *P. vulgaris* roots.
(PDF)

S7 Fig. DEGs of cell wall-related genes during root symbioses.
(PDF)

S8 Fig. DEGs of N metabolism genes during root symbioses.
(PDF)

S9 Fig. Effect of root symbiosis on the nitrogen metabolism pathway in mycorrhized and nodulated roots.
(PDF)

S10 Fig. DEGs of P metabolism genes during root symbioses.
(PDF)

S11 Fig. Effect of root symbiosis on the inositol phosphate metabolism pathway in mycorrhized and nodulated *P. vulgaris* roots.
(PDF)

S1 Table. Primer sequences of *P. vulgaris* genes used to perform RT-qPCR analyses.
(DOCX)

S2 Table. Summary of the number of Ion Proton sequencer reads and BLASTX hits to the *P. vulgaris* genome database.
(DOC)

S3 Table. List of upregulated and downregulated DEGs identified from mycorrhized and nodulated *P. vulgaris* roots.
(XLS)

S4 Table. List significantly enriched GO terms of upregulated and downregulated DEGs identified from mycorrhized and nodulated *P. vulgaris* roots.
(XLS)

S5 Table. Total number of transcription factors of different families that are differentially expressed in mycorrhized and nodulated *P. vulgaris* roots.
(DOCX)

S6 Table. Quantitative expression profiles of unique and overlapping DEGs related to defense, cell wall, N metabolism and P metabolism.
(XLS)

Acknowledgments

Author Contributions

Conceptualization: Manoj-Kumar Arthikala.

Data curation: Kalpana Nanjareddy.

Formal analysis: Kalpana Nanjareddy, Brenda-Mariana Gómez, Lourdes Blanco.

References

1. Remy W, Taylor TN, Hass H, Ker H. Four hundred-million-year-old vesicular-arbuscular mycorrhizae. P Natl Acad Sci USA. 1994; 91:11841–11843.

2. Barea JM, Pozo MJ, Azcón R, Azcon-Aguilar C. Microbial co-operation in the rhizosphere. J Exp Bot. 2005; 56:1761–1778. https://doi.org/10.1093/jxb/eri197 PMID: 15911555

3. Meghvansi MK, Prasad K, Harwani D, Mahna SK. Response of soil bean cultivars toward inoculation with three arbuscular mycorrhizal fungi and *Bradyrhizobium japonicum* in the alluvial soil. Eur J Soil Biol. 2008; 44:316–323.

4. Kaschuk G, Leffelaar PA, Giller KE, Alberton O, Hungria M, Kuyper TW. Responses of legumes to rhizobia and arbuscular mycorrhizal fungi: a meta-analysis of potential photosynthate limitation of symbioses. Soil Biol Biochem. 2010; 42:125–127.

5. Govindarajulu M, Pfeffer PE, Jin HR, Abubaker J, Douds DD, Allen JW, et al. Nitrogen transfer in the arbuscular mycorrhizal symbiosis. Nature. 2005; 435:819–823. https://doi.org/10.1038/nature03610 PMID: 15944705

6. Masson-Boivin C, Giraud E, Perret X, Batut J. Establishing nitrogen-fixing symbiosis with legumes: how many rhizobium recipes? Trends Microbiol. 2009; 17:458–466. https://doi.org/10.1016/j.tim.2009.07.004 PMID: 19766492

7. Smith SE, Smith FA. Roles of arbuscular mycorrhizas in plant nutrition and growth: new paradigms from cellular to ecosystems scales. Annu Rev Plant Biol. 2011; 63:227–250.

8. Besserer A, Puech-Pagès V, Kiefer P, Gomez-Roldan V, Jauneau A, Roy S, et al. Strigolactones stimulate arbuscular mycorrhizal fungi by activating mitochondria. PLoS Biol. 2006; 4:e226. https://doi.org/10.1371/journal.pbio.0040226 PMID: 16787107

9. Maillet F, Poinsot V, Andre´ O, Puech-Page´s V, Haouy A, Gueunier M, et al. Fungal lipochitooligosaccharide symbiotic signals in arbuscular mycorrhiza. Nature. 2011; 469:58–63. https://doi.org/10.1038/nature09622 PMID: 21209659

10. Genre A, Chabaud M, Balzergue C, Puech-Pagès V, Novero M, Rey T, et al. Short-chain chitin oligomers from arbuscular mycorrhizal fungi trigger nuclear Ca^{2+} spiking in *Medicago truncatula* roots and their production is enhanced by strigolactone. New Phytol. 2013; 198:179–189.

11. Broughton WJ, Jabbouri S, Perret X. Keys to symbiotic harmony. J Bacteriol. 2000; 182:5641–5652. PMID: 11004160

12. Oldroyd GED, Downie JA. Coordinating nodule morphogenesis with rhizobial infection in legumes. Annu Rev Plant Biol. 2008; 59:519–546. https://doi.org/10.1146/annurev.arplant.59.032607.092839 PMID: 18444906

13. Kistner C, Winzer T, Pitzschke A, Mulder L, Sato S, Kaneko T, et al. Seven *Lotus japonicus* genes required for transcriptional reprogramming of the root during fungal and bacterial symbiosis. Plant Cell. 2005; 17:2217–2229. https://doi.org/10.1105/tpc.105.032714 PMID: 15980262

14. Rogers C, Oldroyd GE. Synthetic biology approaches to engineering the nitrogen symbiosis in cereals. J Exp Bot. 2014; 65:1939–1946. https://doi.org/10.1093/jxb/eru098 PMID: 24687978

15. Smit P, Raedts J, Portyanko V, Debellé F, Gough C, Bisseling T, et al. NSP1 of the GRAS protein family is essential for rhizobial Nod factor-induced transcription. Science. 2005; 308:1789–1791. https://doi.org/10.1126/science.1111025 PMID: 15961669

16. Kaló P, Gleason C, Edwards A, Marsh J, Mitra RM, Hirsch S, et al. Nodulation signaling in legumes requires NSP2, a member of the GRAS family of transcriptional regulators. Science. 2005; 308:1786–1789. https://doi.org/10.1126/science.1110951 PMID: 15961668

17. Gobbato E, Marsh JF, Vernié T, Wang E, Maillet F, Kim J, et al. A GRAS-type transcription factor with a specific function in mycorrhizal signaling. Curr Biol. 2012; 22:2236–2241. https://doi.org/10.1016/j.cub.2012.09.044 PMID: 23122845

18. Murray JD, Cousins DR, Jackson KJ, Liu C. Signaling at the Root Surface: The Role of Cutin Monomers in Mycorrhization. Molecular Plant. 2013; 6:1381–1383. https://doi.org/10.1093/mp/sst090 PMID: 23935010

19. Cerri MR, Frances L, Laloum T, Auriac MC, Niebel A, Oldroyd GE, et al. *Medicago truncatula* ERN transcription factors: regulatory interplay with NSP1/NSP2 GRAS factors and expression dynamics throughout rhizobial infection. Plant Physiol. 2012; 160:2155–2172. https://doi.org/10.1104/pp.112.203190 PMID: 23077241

20. Marsh JF, Rakocevic A, Mitra RM, Brocard L, Sun J, Eschstruth A, et al. *Medicago truncatula* NIN Is Essential for Rhizobial-Independent Nodule Organogenesis Induced by Autoactive Calcium/Calmodulin-Dependent Protein Kinase. Plant Physiol. 2007; 144:324–335. https://doi.org/10.1104/pp.106.093021 PMID: 17369436

21. Soyano T, Kouchi H, Hirota A, Hayashi M. NODULE INCEPTION Directly Targets NF-Y Subunit Genes to Regulate Essential Processes of Root Nodule Development in *Lotus japonicus*. PLoS Genet. 2013; 9:e1003352. https://doi.org/10.1371/journal.pgen.1003352 PMID: 23555278

22. Murray JD, Karas BJ, Sato S, Tabata S, Amyot L, Szczyglowski K. A cytokinin perception mutant colonized by *Rhizobium* in the absence of nodule organogenesis. Science. 2007; 315:101–104. https://doi.org/10.1126/science.1132514 PMID: 17110535

23. Tirichine L, Sandal N, Madsen LH, Radutoiu S, Albrektsen AS, Sato S, et al. A gain-of-function mutation in a cytokinin receptor triggers spontaneous root nodule organogenesis. Science. 2007; 315:104–107. https://doi.org/10.1126/science.1132397 PMID: 17110537

24. Bapaume L, Reinhardt D. How membranes shape plant symbioses: signaling and transport in nodulation and arbuscular mycorrhiza. Front Plant Sci. 2012; 3:223. https://doi.org/10.3389/fpls.2012.00223 PMID: 23060892

25. Zanetti ME, Blanco FA, Beker MP, Battaglia M, Aguilar OM. A *C* Subunit of the Plant Nuclear Factor NF-Y Required for Rhizobial Infection and Nodule Development Affects Partner Selection in the Common Bean-*Rhizobium etli* Symbiosis. Plant Cell. 2010; 12:4142–4157.

26. Sánchez-López R, Jáuregui D, Nava N, Alvarado-Affantranger X, Montiel J, Santana O, et al. Down-regulation of SymRK correlates with a deficiency in vascular bundle development in *Phaseolus vulgaris* nodules. Plant Cell Environ. 2011; 34:2109–2121. https://doi.org/10.1111/j.1365-3040.2011.02408.x PMID: 21848862

27. Islas-Flores T, Guillén G, Alvarado-Affantranger X, Lara-Flores M, Sánchez F, Villanueva MA. PvRACK1 loss-of-function impairs cell expansion and morphogenesis in *Phaseolus vulgaris* L. root nodules. Mol Plant Microbe Interact. 2011; 24:819–826. https://doi.org/10.1094/MPMI-11-10-0261 PMID: 21425924

28. Montiel J, Nava N, Cárdenas L, Sánchez-López R, Arthikala MK, Santana O, et al. A *Phaseolus vulgaris* NADPH oxidase gene is required for root infection by Rhizobia. Plant Cell Physiol. 2012; 53:1751–1767. https://doi.org/10.1093/pcp/pcs120 PMID: 22942250

29. Barraza A, Estrada-Navarrete G, Rodriguez-Alegria ME, Lopez-Munguia A, Merino E, Quinto C, et al. Down-regulation of PvTRE1 enhances nodule biomass and bacteroid number in the common bean. New Phytol. 2013; 197:194–206. https://doi.org/10.1111/nph.12002 PMID: 23121215

30. Rodriguez-López J, Martínez-Centeno C, Padmanaban A, Guillén G, Olivares JE, Stefano G, et al. Nodulin 22, a novel small heat-shock protein of the endoplasmic reticulum, is linked to the unfolded protein response in common bean. Mol Plant Microbe Interact. 2014; 27:18–29. https://doi.org/10.1094/MPMI-07-13-0200-R PMID: 24073881

31. Battaglia M, Ripodas C, Clua J, Baudin M, Aguilar OM, Niebel A, et al. A Nuclear Factor Y Interacting Protein of the GRAS Family Is Required for Nodule Organogenesis, Infection Thread Progression, and Lateral Root Growth. Plant Physiol. 2014; 164:1430–1442. https://doi.org/10.1104/pp.113.230896 PMID: 24424321

32. Nanjareddy K, Blanco L, Arthikala MK, Alvarado-Affantranger X, Quinto C, Sánchez F, et al. A Legume TOR Protein Kinase Regulates *Rhizobium* Symbiosis and Is Essential for Infection and

Nodule Development. Plant Physiol. 2016; 172:2002–2020. https://doi.org/10.1104/pp.16.00844 PMID: 27698253

33. Arthikala MK, Montiel J, Nava N, Santana O, Sánchez-López R, Cárdenas L, et al. PvRbohB negatively regulates *Rhizophagus irregularis* colonization in *Phaseolus vulgaris*. Plant Cell Physiol. 2013; 54:1391–13402. https://doi.org/10.1093/pcp/pct089 PMID: 23788647

34. Arthikala MK, Sánchez-López R, Nava N, Santana O, Cárdenas L, Quinto C. RbohB, a *Phaseolus vulgaris* NADPH oxidase gene, enhances symbiosome number, bacteroid size, and nitrogen fixation in nodules and impairs mycorrhizal colonization. New Phytol. 2014; 202:886–900. https://doi.org/10.1111/nph.12714 PMID: 24571730

35. Estrada-Navarrete G, Cruz-Mireles N, Lascano R, Alvarado-Affantranger X, Hernàndez A, Barraza A, et al. An autophagy-related kinase is essential for the symbiotic relationship between *Phaseolus vulgaris* and both rhizobia and arbuscular mycorrhizal fungi. Plant Cell. 2016; 28:2326–2341.

36. Deguchi Y, Banba M, Shimoda Y, Chechetka SA, Suzuri R, Okusako Y, et al. Transcriptome Profiling of *Lotus japonicus* Roots During Arbuscular Mycorrhiza Development and Comparison with that of Nodulation. DNA Research: An International Journal for Rapid Publication of Reports on Genes and Genomes. 2007; 14:117–133.

37. Tromas A, Parizot B, Diagne N, Champion A, Hocher V, Cissoko M, et al. Heart of endosymbioses: transcriptomics reveals a conserved genetic program among arbuscular mycorrhizal, actinorhizal and legume-rhizobial symbioses. PLoS One. 2012; 7:e44742. https://doi.org/10.1371/journal.pone.0044742 PMID: 22970303

38. Roux B, Rodde N, Jardinaud MF, Timmers T, Sauviac L, Cottret L, et al. An integrated analysis of plant and bacterial gene expression in symbiotic root nodules using laser-capture microdissection coupled to RNA sequencing. Plant J. 2014; 77:817–837. https://doi.org/10.1111/tpj.12442 PMID: 24483147

39. Alves-Carvalho S, Aubert G, Carrère S, Cruaud C, Brochot AL, Jacquin F, et al. Full-length de novo assembly of RNA-seq data in pea (*Pisum sativum* L.) provides a gene expression atlas and gives insights into root nodulation in this species. Plant J. 2015; 84:1–19. https://doi.org/10.1111/tpj.12967 PMID: 26296678

40. Wang Z, Gerstein M, Snyder M. RNA-Seq: a revolutionary tool for transcriptomics. Nat Rev Genet. 2009; 10:57–63. https://doi.org/10.1038/nrg2484 PMID: 19015660

41. Takeda N, Handa Y, Tsuzuki S, Kojima M, Sakakibara H, Kawaguchi M. Gibberellins Interfere with Symbiosis Signaling and Gene Expression and Alter Colonization by Arbuscular Mycorrhizal Fungi in *Lotus japonicus*. Plant Physiol. 2015; 167:545–57. https://doi.org/10.1104/pp.114.247700 PMID: 25527715

42. Xue L, Cui H, Buer B, Vijayakumar V, Delaux PM, Junkermann S, et al. Network of GRAS transcription factors involved in the control of arbuscule development in *Lotus japonicus*. Plant Physiol. 2015; 167:854–871. https://doi.org/10.1104/pp.114.255430 PMID: 25560877

43. Broughton WJ, Dilworth MJ. Control of leghemoglobin synthesis in snake beans. Biochem J. 1971; 125:1075–1080. PMID: 5144223

44. Ceballos I, Ruiz M, Fernández C, Peña R, Rodríguez A, Sanders IR. The *in vitro* mass-produced model mycorrhizal fungus, *Rhizophagus irregularis*, significantly increases yields of the globally important food security crop cassava. PLoS One. 2013; 8:e70633. https://doi.org/10.1371/journal.pone.0070633 PMID: 23950975

45. Martínez-Romero E, Segovia L, Mercante FM, Franco AA, Graham P, Pardo MA. *Rhizobium tropici*: a novel species nodulating *Phaseolus vulgaris* L. beans and *Leucaena sp.* trees. Int J Syst Bacteriol. 1991; 41:417–426. https://doi.org/10.1099/00207713-41-3-417 PMID: 1715738

46. Smith SE, Smith FA, Jakobsen I. Mycorrhizal fungi can dominate phosphate supply to plants irrespective of growth responses. Plant Physiol. 2003; 133:16–20. PMID: 12970469

47. Nanjareddy K, Blanco L, Arthikala MK, Affantrange XA, Sánchez F, Lara M. Nitrate regulates rhizobial and mycorrhizal symbiosis in common bean (*Phaseolus vulgaris* L.). J Integr Plant Biol. 2014; 56:281–298. https://doi.org/10.1111/jipb.12156 PMID: 24387000

48. McGonigle TP, Millers MH, Evans DG, Fairchild GL, Swan JA. A new method which gives an objective measure of colonization of roots by vesicular-arbuscular mycorrhizal fungi. New Phytol. 1990; 115:495–501.

49. Miller RO. Nitric-perchloric acid wet digestion in an open vessel. Handbook of Reference Methods for Plant Analysis. 1998;57–61.

50. Ramírez M, Valderrama B, Arredondo-Peter R, Soberón M, Mora J, Hernández G. *Rhizobium etli* genetically engineered for the heterologous expression of *Vitreoscilla* sp. hemoglobin: effects on free-living and symbiosis. Mol Plant-Microbe Interact. 1999; 12:1008–1015.

51. Bustin SA, Benes V, Garson JA, Hellemans J, Huggett J, Kubista M, et al. The MIQE guidelines: mini-mum information for publication of quantitative real-time PCR experiments. Clin Chem. 2009; 55: 611–622. https://doi.org/10.1373/clinchem.2008.112797 PMID: 19246619

52. Vandesompele J, De Preter K, Pattyn F, Poppe B, Van Roy N, De Paepe A, et al. Accurate normaliza-tion of real-time quantitative RT-PCR data by geometric averaging of multiple internal reference genes. Genome Biol. 2002; 3:research0034.1–0034.11.

53. Kashofer K, Viertler C, Pichler M, Zatloukal K. Quality Control of RNA Preservation and Extraction from Paraffin-Embedded Tissue: Implications for RT-PCR and Microarray Analysis. PLoS One. 2013; 8:e70714. https://doi.org/10.1371/journal.pone.0070714 PMID: 23936242

54. Du Zhou, Zhou Xin, Ling Yi, Zhang Z Zhen Su. agriGO: a GO analysis toolkit for the agricultural com-munity. Nucl Acids Res. 2010; 38:W64–W70. https://doi.org/10.1093/nar/gkq310 PMID: 20435677

55. Eisen MB, Spellman PT, Brown PO, Botstein D. Cluster analysis and display of genome-wide expres-sion patterns. P Natl Acad Sci USA. 1998; 95:14863–14868.

56. Supek F, Bošnjak M, Škunca N, Šmuc T. REVIGO summarizes and visualizes long lists of Gene Ontology terms. PLoS One. 2011; 6:e21800. https://doi.org/10.1371/journal.pone.0021800 PMID: 21789182

57. Kanehisa M. KEGG bioinformatics resource for plant genomics and metabolomics. Methods Mol Biol. 2016; 1374:55–70. https://doi.org/10.1007/978-1-4939-3167-5_3 PMID: 26519400

58. Hirsch S, Kim J, Muñoz A, Heckmann AB, Downie JA, Oldroyd GE. GRAS proteins form a DNA bind-ing complex to induce gene expression during nodulation signaling in *Medicago truncatula*. Plant Cell. 2009; 21:545–557. https://doi.org/10.1105/tpc.108.064501 PMID: 19252081

59. Jones JD, Dangl JL. The plant immune system. Nature. 2006; 444:323–329. https://doi.org/10.1038/nature05286 PMID: 17108957

60. Oldroyd GE. Speak, friend, and enter: signaling systems that promote beneficial symbiotic associa-tions in plants. Nat Rev Microbiol. 2013; 11:252–263. https://doi.org/10.1038/nrmicro2990 PMID: 23493145

61. Jiang Y and Yu D. WRKY57 regulates JAZ genes transcriptionally to compromise *Botrytis cinerea* resistance in *Arabidopsis thaliana*. Plant Physiol. 2016; 171:2771–2782. https://doi.org/10.1104/pp.16.00747 PMID: 27268959

62. Suza WP, Staswick PE. The role of JAR1 in Jasmonoyl-L: -isoleucine production during *Arabidopsis* wound response. Planta. 2008; 227:1221–1232. https://doi.org/10.1007/s00425-008-0694-4 PMID: 18247047

63. Underwood W. The Plant Cell Wall: A Dynamic Barrier Against Pathogen Invasion. Front Plant Sci. 2012; 3:85. https://doi.org/10.3389/fpls.2012.00085 PMID: 22639669

64. Rich MK, Schorderet M, Reinhardt D. The role of the cell wall compartment in mutualistic symbioses of plants. Front Plant Sci. 2014; 5:238. https://doi.org/10.3389/fpls.2014.00238 PMID: 24917869

65. Kaewthai N, Gendre D, Eklof JM, Ibatullin FM, Ezcurra I, Bhalerao RP, et al. Group III-A XTH genes of *Arabidopsis* encode predominant xyloglucan endohydrolases that are dispensable for normal growth. Plant Physiol. 2013; 161:440–454. https://doi.org/10.1104/pp.112.207308 PMID: 23104861

66. Lionetti V, Fabri E, De Caroli M, Hansen AR, Willats WG, Piro G, et al. Three pectin methyl esterase inhibitors protect cell wall integrity for immunity to *Botrytis*. Plant Physiol. 2017;doi: https://doi.org/10.1104/pp.16.01185 PMID: 28082716

67. Wang Y, Wang L, Zou Y, Chen L, Cai Z, Zhang S, et al. Soybean miR172c Targets the Repressive AP2 Transcription Factor NNC1 to Activate ENOD40 Expression and Regulate Nodule Initiation. Plant Cell. 2014; 26:4782–4801. https://doi.org/10.1105/tpc.114.131607 PMID: 25549672

68. Asamizu E, Shimoda Y, Kouchi H, Tabata S, Sato S. A Positive Regulatory Role for LjERF1 in the Nodulation Process Is Revealed by Systematic Analysis of Nodule-Associated Transcription Factors of *Lotus japonicus*. Plant Physiol. 2008; 147:2030–2040. https://doi.org/10.1104/pp.108.118141 PMID: 18567832

69. Vernié T, Moreau S, de Billy F, Plet J, Combier J- P, Rogers C, et al. EFD Is an ERF Transcription Fac-tor Involved in the Control of Nodule Number and Differentiation in *Medicago truncatula*. Plant Cell. 2008; 20:2696–2713. https://doi.org/10.1105/tpc.108.059857 PMID: 18978033

70. Zucchero JC, Caspi M, Dunn K. ngl9: a third MADS box gene expressed in alfalfa root nodules. Mol Plant Microbe Interact. 2001; 14:1463–1467. https://doi.org/10.1094/MPMI.2001.14.12.1463 PMID: 11768543

71. Azarakhsh M, Kirienko AN, Zhukov VA, Lebedeva MA, Dolgikh EA, Lutova LA. KNOTTED1-LIKE HOMEOBOX 3: a new regulator of symbiotic nodule development. J Exp Bot. 2015; 66:7181–7195. https://doi.org/10.1093/jxb/erv414 PMID: 26351356

72. Smith PMC, Atkins CA. Purine biosynthesis. Big in cell division, even bigger in nitrogen assimilation. Plant Physiol. 2002; 128:793–802. https://doi.org/10.1104/pp.010912 PMID: 11891236

73. Zrenner R, Stitt M, Sonnewald U, Boldt R. Pyrimidine and purine biosynthesis and degradation in plants. Annu Rev Plant Biol. 2006; 57:805–836. https://doi.org/10.1146/annurev.arplant.57.032905.105421 PMID: 16669783

74. Theodorou ME, Plaxton WC. Metabolic adaptations of plant respiration to nutritional phosphate deprivation. Plant Physiol. 1993; 101:339–344. PMID: 12231689

75. Frenzel A, Manthey K, Perlick AM, Meyer F, Pühler A, Küster H, et al. Combined transcriptome profiling reveals a novel family of arbuscular mycorrhizal-specific *Medicago truncatula* lectin genes. Mol Plant Microbe Interact. 2005; 8:771–782.

76. Frenzel A, Tiller N, Hause B, Krajinski F. The conserved arbuscular mycorrhiza-specific transcription of the secretory lectin MtLec5 is mediated by a short upstream sequence containing specific protein binding sites. Planta. 2006; 224:792–800. https://doi.org/10.1007/s00425-006-0262-8 PMID: 16596411

77. De Hoff PL, Brill LM, Hirsch AM. Plant lectins: the ties that bind in root symbiosis and plant defense. Mol Genet Genomics. 2009; 282:1–15. https://doi.org/10.1007/s00438-009-0460-8 PMID: 19488786

78. Williams SP, Gillaspy GE, Perera IY. Biosynthesis and possible functions of inositol pyrophosphates in plants. Front Plant Sci. 2015; 6:67. https://doi.org/10.3389/fpls.2015.00067 PMID: 25729385

79. Kuo HF, Chang TY, Chiang SF, Wang WD, Charng YY, Chiou TJ. *Arabidopsis* inositol pentakisphosphate 2-kinase, AtIPK1, is required for growth and modulates phosphate homeostasis at the transcriptional level. Plant J. 2014; 80:503–515. https://doi.org/10.1111/tpj.12650 PMID: 25155524

80. Ding Y, Ndamukong I, Zhao Y, Xia Y, Riethoven JJ, Jones DR, et al. Divergent functions of the myotubularin (MTM) homologs AtMTM1 and AtMTM2 in *Arabidopsis thaliana*: evolution of the plant MTM family. Plant J. 2012; 70:866–878. https://doi.org/10.1111/j.1365-313X.2012.04936.x PMID: 22324391

81. Arthikala MK, Nava N, Quinto C. Effect of Rhizobium and arbuscular mycorrhizal fungi inoculation on electrolyte leakage in *Phaseolus vulgaris* roots overexpressing RbohB. Plant Signal Behav. 2015; 10: e1011932. https://doi.org/10.1080/15592324.2015.1011932 PMID: 25946118

82. Ramírez M, Graham MA, Blanco-López L, Silvente S, Medrano-Soto A, Blair MW, et al. Sequencing and analysis of common bean ESTs. Building a foundation for functional genomics. Plant Physiol. 2005; 137:1211–1227. https://doi.org/10.1104/pp.104.054999 PMID: 15824284

83. O'Rourke JA, Iniguez LP, Fu F, Bucciarelli B, Miller SS, Jackson SA, et al. An RNA-Seq based gene expression atlas of the common bean. BMC Genomics. 2014; 15:866. https://doi.org/10.1186/1471-2164-15-866 PMID: 25283805

84. Handa Y, Nishide H, Takeda N, Suzuki Y, Kawaguchi M, Saito K. RNA-seq Transcriptional Profiling of an Arbuscular Mycorrhiza Provides Insights into Regulated and Coordinated Gene Expression in *Lotus japonicus* and *Rhizophagus irregularis*. Plant Cell Physiol. 2015; 56:1490–1511. https://doi.org/10.1093/pcp/pcv071 PMID: 26009592

85. Gomez SK, Javot H, Deewatthanawong P, Torres-Jerez I, Tang Y, Blancaflor E, et al. *Medicago truncatula* and *Glomus intraradices* gene expression in cortical cells harboring arbuscules in the arbuscular mycorrhizal symbiosis. BMC Plant Biol. 2009; 9:10. https://doi.org/10.1186/1471-2229-9-10 PMID: 19161626

86. Guether M, Balestrini R, Hannah M, He J, Udvardi MK, Bonfante P. Genome-wide reprogramming of regulatory networks, transport, cell wall and membrane biogenesis during arbuscular mycorrhizal symbiosis in *Lotus japonicus*. New Phytol. 2009; 182:200–212. https://doi.org/10.1111/j.1469-8137.2008.02725.x PMID: 19192192

87. Hogekamp C, Arndt D, Pereira P, Becker JD, Hohnjec N, Küster H. Laser microdissection unravels cell-type-specific transcription in arbuscular mycorrhizal roots, including CAAT-Box transcription factor gene expression correlating with fungal contact and spread. Plant Physiol. 2011; 157:2023–2043. https://doi.org/10.1104/pp.111.186635 PMID: 22034628

88. Gaude N, Bortfeld S, Duensing N, Lohse M, Krajinski F. Arbuscule-containing and non-colonized cortical cells of mycorrhizal roots undergo a massive and specific reprogramming during arbuscular mycorrhizal development. Plant J. 2012; 69:510–528. https://doi.org/10.1111/j.1365-313X.2011.04810.x PMID: 21978245

89. Hogekamp C, Küster H. A roadmap of cell-type specific gene expression during sequential stages of the arbuscular mycorrhiza symbiosis. BMC Genomics. 2013; 14:306. https://doi.org/10.1186/1471-2164-14-306 PMID: 23647797

90. Larrainzar E, Riely BK, Kim SC, Carrasquilla-Garcia N, Yu H- J, Hwang HJ, et al. Deep Sequencing of the *Medicago truncatula* Root Transcriptome Reveals a Massive and Early Interaction Between

Nodulation Factor and Ethylene Signals. Plant Physiol. 2015; 169:233–265. https://doi.org/10.1104/pp.15.00350 PMID: 26175514

91. Boscari A, del Giudice J, Ferrarini A, Venturini L, Zaffini A- L, Delledonne M, et al. Expression Dynamics of the *Medicago truncatula* Transcriptome during the Symbiotic Interaction with *Sinorhizobium meliloti*: Which Role for Nitric Oxide? Plant Physiol. 2013; 161:425–439. https://doi.org/10.1104/pp.112.208538 PMID: 23136381

92. David R, Itzhaki H, Ginzberg I, Gafni Y, Galili G, Kapulnik Y. Suppression of tobacco basic chitinase gene expression in response to colonization by the arbuscular mycorrhizal fungus *Glomus intraradices*. Mol Plant Microbe Interact. 1998; 11:489–497. https://doi.org/10.1094/MPMI.1998.11.6.489 PMID: 9612947

93. Marone D, Russo MA, Laidò G, De Leonardis AM. Mastrangelo AM Plant nucleotide binding site-leucine-rich repeat (NBS-LRR) genes: active guardians in host defense responses. Int J Mol Sci. 2013; 14:7302–7326. https://doi.org/10.3390/ijms14047302 PMID: 23549266

94. Plett JM, Khachane A, Ouassou M, Sundberg B, Kohler A, Martin F. Ethylene and jasmonic acid act as negative modulators during mutualistic symbiosis between *Laccaria bicolor* and *Populus* roots. New Phytol. 2014; 202:270–286. https://doi.org/10.1111/nph.12655 PMID: 24383411

95. Ferrari S, Plotnikova JM, De Lorenzo G, Ausubel FM. *Arabidopsis* local resistance to *Botrytis cinerea* involves salicylic acid and camalexin and requires EDS4 and PAD2, but not SID2, EDS5 or PAD4. Plant J. 2003; 35:193–205. PMID: 12848825

96. Kawamura Y, Takenaka S, Hase S, Kubota M, Ichinose Y, Kanayama Y, et al. Enhanced defense responses in *Arabidopsis* induced by the cell wall protein fractions from *Pythium oligandrum* require SGT1, RAR1, NPR1, and JAR1. Plant Cell Physiol. 2009; 50:924–34. https://doi.org/10.1093/pcp/pcp044 PMID: 19304739

97. Aslam SN, Newman MA, Erbs G, Morrissey KL, Chinchilla D, Boller T, et al. Bacterial polysaccharides suppress induced innate immunity by calcium chelation. Curr Biol. 2008; 18:1078–1083. https://doi.org/10.1016/j.cub.2008.06.061 PMID: 18639458

98. Cosgrove DJ. Growth of the plant cell wall. Nat Rev Mol Cell Biol. 2005; 6:850–861. https://doi.org/10.1038/nrm1746 PMID: 16261190

99. Maldonado-Mendoza IE, Dewbre GR, Blaylock L, Harrison MJ. Expression of a xyloglucan endotransglucosylase/hydrolase gene, *Mt-XTH1*, from *Medicago truncatula* is induced systemically in mycorrhizal roots. Gene. 2005; 345:191–197. https://doi.org/10.1016/j.gene.2004.10.028 PMID: 15716119

100. Guo W, Zhao J, Li X, Qin L, Yan X, Liao H. A soybean *β*-expansin gene *GmEXPB2* intrinsically involved in root system architecture responses to abiotic stresses. Plant J. 2011; 66:541–552. https://doi.org/10.1111/j.1365-313X.2011.04511.x PMID: 21261763

101. Marowa P, Ding A, Kong Y. Expansins: roles in plant growth and potential applications in crop improvement. Plant Cell Rep. 2016; 35:949–965. https://doi.org/10.1007/s00299-016-1948-4 PMID: 26888755

102. Diaz C, Lemaitre T, Christ A, Azzopardi M, Kato Y, Sato F, et al. Nitrogen recycling and remobilization are differentially controlled by leaf senescence and development stage in *Arabidopsis* under low nitrogen nutrition. Plant Physiol. 2008; 147:1437–1449. https://doi.org/10.1104/pp.108.119040 PMID: 18467460

103. Miller AJ, Fan X, Shen Q, Smith SJ. Amino acids and nitrate as signals for the regulation of nitrogen acquisition. J Exp Bot. 2008; 59:111–119. https://doi.org/10.1093/jxb/erm208 PMID: 18093964

104. Combier JP, Frugier F, De Billy F, Boualem A, El-Yahyaoui F, Moreau S, et al. MtHAP2-1 is a key transcriptional regulator of symbiotic nodule development regulated by microRNA169 in *Medicago truncatula*. Genes Dev. 2006; 20:3084–3088. https://doi.org/10.1101/gad.402806 PMID: 17114582

105. Laloum T, Baudin M, Frances L, Lepage A, Billault-Penneteau B, Cerri MR, et al. Two CCAAT box-binding transcription factors redundantly regulate early steps of the legume-rhizobia endosymbiosis. Plant J. 2014; 79:757–768. https://doi.org/10.1111/tpj.12587 PMID: 24930743

106. Laporte P, Lepage A, Fournier J, Catrice O, Moreau S, Jardinaud MF, et al. The CCAAT box-binding transcription factor NF-YA1 controls rhizobial infection. J Exp Bot. 2014; 65:481–494. https://doi.org/10.1093/jxb/ert392 PMID: 24319255

107. Smith SE, Jakobsen I, Grønlund M, Smith FA. Roles of Arbuscular Mycorrhizas in Plant Phosphorus Nutrition: Interactions between Pathways of Phosphorus Uptake in Arbuscular Mycorrhizal Roots Have Important Implications for Understanding and Manipulating Plant Phosphorus Acquisition. Plant Physiol. 2011; 156:1050–1057. https://doi.org/10.1104/pp.111.174581 PMID: 21467213

108. Cheng Y, Zhou W, El sheery NI, Peters C, Li M, Wang X, et al. Characterization of the *Arabidopsis* glycerophosphodiester phosphodiesterase (GDPD) family reveals a role of the plastid-localized AtGDPD1 in maintaining cellular phosphate homeostasis under phosphate starvation. Plant J. 2011; 66:781–795. https://doi.org/10.1111/j.1365-313X.2011.04538.x PMID: 21323773